Figure 42: Satellite image of Tractor Beach with surveys extents undertaken and locations of samples collected by year.

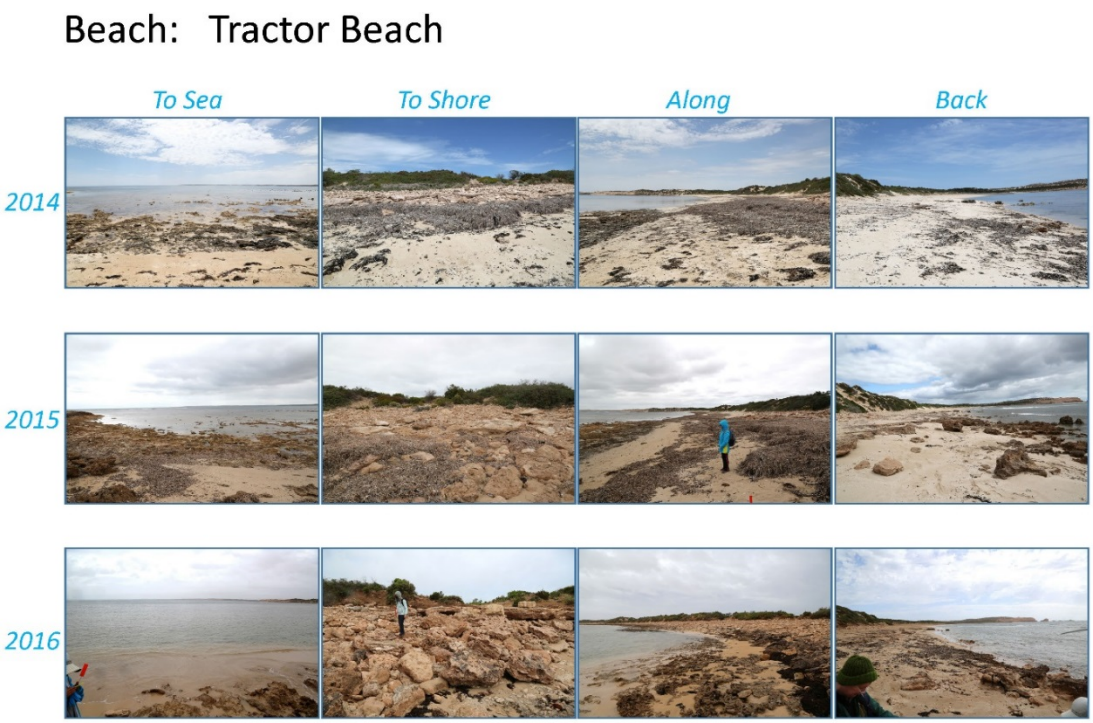

Figure 43: Images taken of the beach for each year for the Tractor Beach surveys.

Beach Summary Data

[sample types include asphaltite, tarball and resinite]

Beach Character Chart

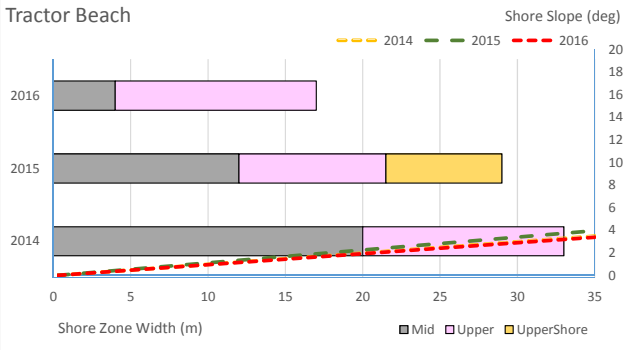

Sample Loadings per 100m Chart

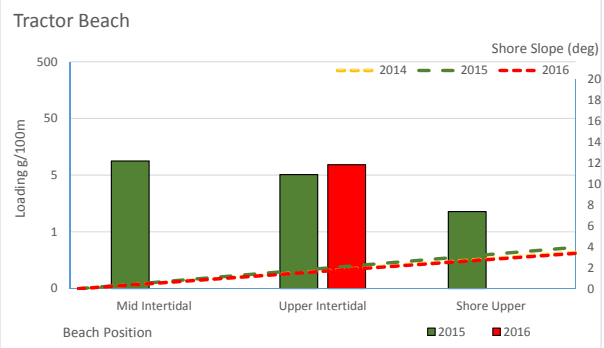

Asphaltite Frequency Chart

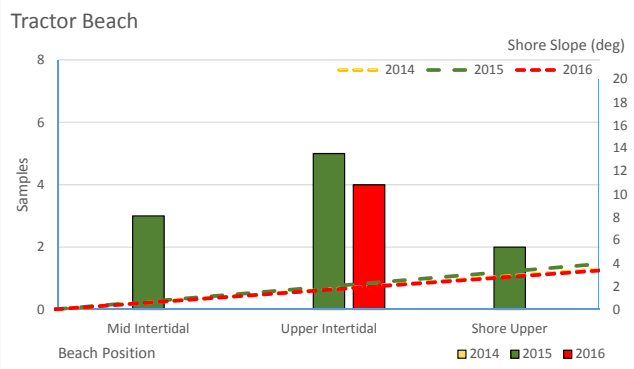

Tarball Frequency Chart

No tarballs found on this beach

Debris Loadings Chart

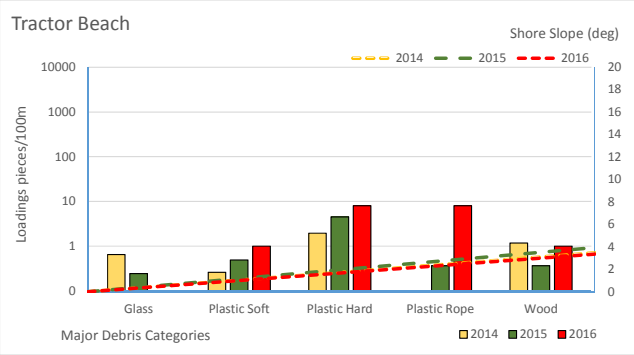

Figure 44: Compilation of beach survey data graphs Tractor Beach.

Dogfence Beach

Dogfence Beach is located on the northwest margin of Eyre Peninsula and as such is a comparator beach to Tractor Beach. It is classified as a wave-dominated high energy double bar dissipative beach (http://www.ozcoasts.gov.au; Short, 2012). Once again, this beach had not previously been surveyed for asphaltites and tarballs. The 2 km of beach surveyed comprises the southeastern end of a straight southwest-facing uninterrupted 20 km long beach (Figure 45). At the south eastern end of the surveyed section is a bluff which forms the end of the beach.

Shoreline photographs from each year show at the macro scale that stranded materials accumulate along wrack lines (Figure 46) along the beach and that the beach morphology does not appear to change considerably.

The beach had variable widths of between 65 and 31 m (dependant on survey year) that that declined in successive years between 2014 and 2016 (Figure 47). It has a low slope angle of between 1.8 and 3.7 degrees (Figure 47) and is composed of fine white sand. The back beach is characterised by a series of large sand dunes.

This beach was the source of both tarballs and asphaltites. Tarball samples were collected from the upper intertidal and upper shoreline zones in all years, whereas asphaltites were only encountered during the 2016 survey (Figure 47). The tarballs collected in 2014 were generally larger than those found in subsequent years. The tarballs collected from the upper intertidal zone in 2015 and 2016 were generally larger than those on the upper shore (based on loadings data: Figure 47) possibly suggesting some degree of sorting/winnowing on deposition.

As at Beachport Conservation Park and Tractor Beach, the majority of the samples collected here were found at the south eastern end of the beach within 250 m of the bluff. This suggests that materials accumulate in this location as a result of longshore drift to the southeast (Figure 45). As such they could represent the materials swept from the 20 km of beach catchment. Exceptions to this pattern are the 2015 tarball stranding sites which, whilst most prevalent at the southeastern end of the beach, were also disributed at irregular intervals to the northwest along the beach transect (Figure 45). It is not possible to ascertain if this was also the case in 2016 due to the shorter survey transect. It should be noted that, as at Number 1 & 2 Rocks, large amounts of anthropogenic materials were found which was surprising considering its remote location. This suggests that materials are conserved on the beach once they arrive but are also transported to the southeastern end of the beach by longshore drift.

The length of Dogfence Beach, combined with its orientation toward the direction of winter storms and onshore winds, means that it is likely to receive materials from a variety of sources. Both surface drifters affected strongly by windage, and those which are less affected by windage, could be expected to accumulate on the beach. Thus, due to the large collection area of this beach it is likely that the abundance of materials is over represented with respect to other beaches (e.g. embayments) with more restricted catchments.

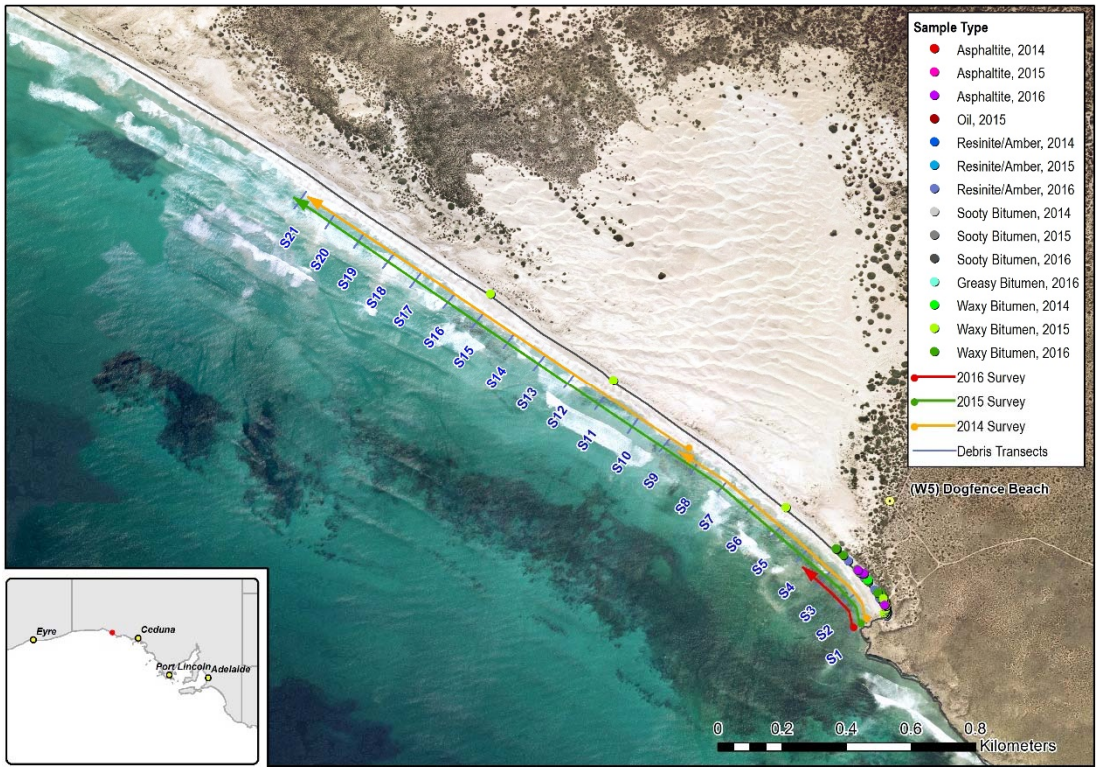

Figure 45: Satellite image of Dogfence Beach with surveys extents undertaken and locations of samples collected by year.

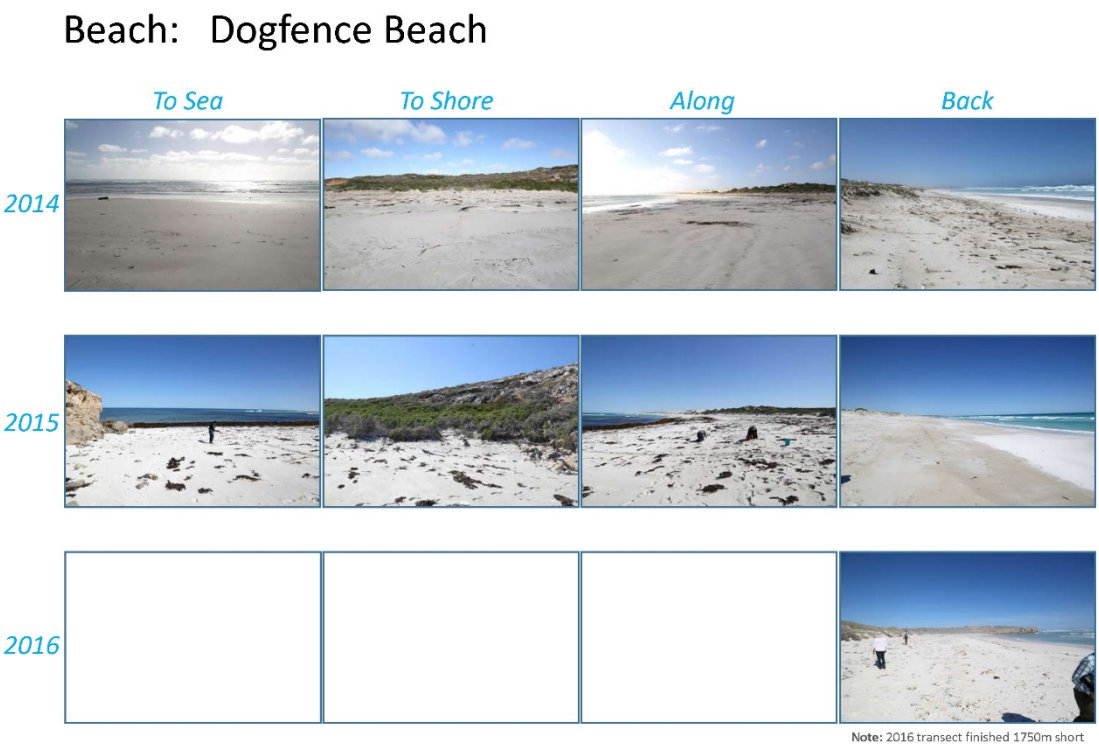

Figure 46: Images taken of the beach for each year for the Dogfence Beach surveys.

Beach Summary Data

[sample types include asphaltite, tarball and resinite]

Beach Character Chart

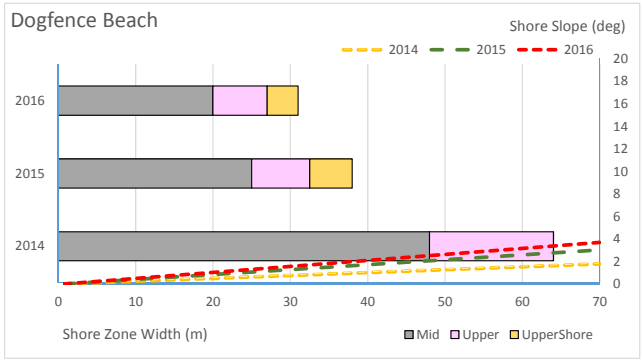

[2016 shore widths estimated]

Sample Loadings per 100m Chart

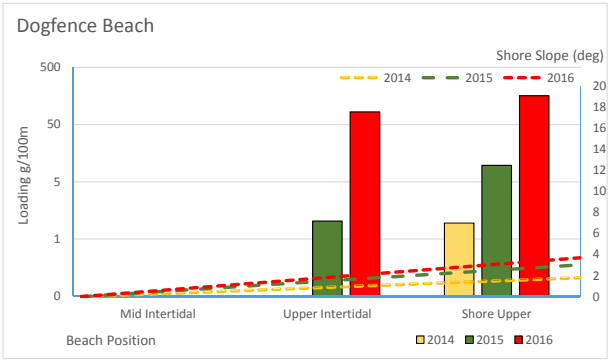

Asphaltite Frequency Chart

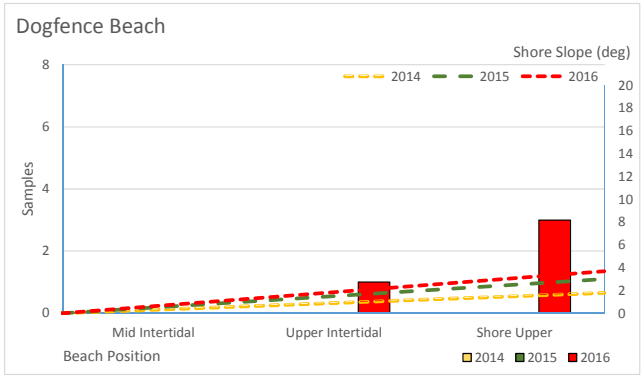

Tarball Frequency Chart

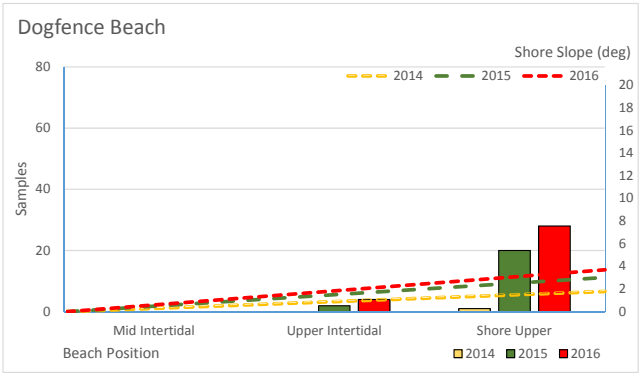

Debris Loadings Chart

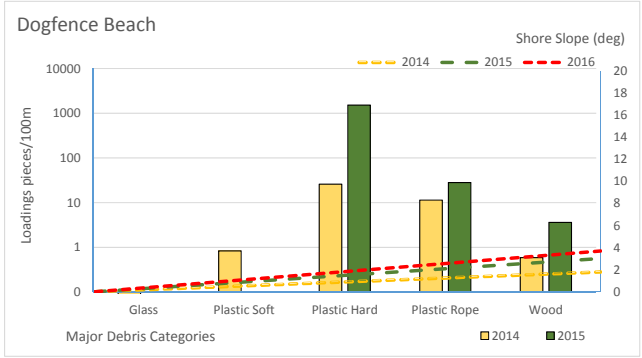

Figure 47: Compilation of beach survey data graphs Dogfence Beach.

Conceptual processes for beach strandings

The detailed study of these four example beaches has identified a number of processes that when combined with the beach type could contribute to the retention and accumulation of materials on low-angle beaches. These are best summarised through simplified conceptual diagrams (Figure 48 and Figure 49). For open aspect beaches, where offshore waves are not funneled onto the beach, waves along with tarballs and asphaltites can arrive from a range of directions (Figure 48). Where the prevailing wave direction is not parallel to the beach, the action of longshore drift will facilitate the movement of materials towards one end of the beach (Figure 48). For most of the southwest-facing beaches in this study, this movement will be to the southeast leading to accumulation of materials at one end of the beach. In addition, the shoreline currents will create rips at the end of these beaches to transport water out of the beaches, permitting the loss of materials that reenter the water in these locations (Figure 48).

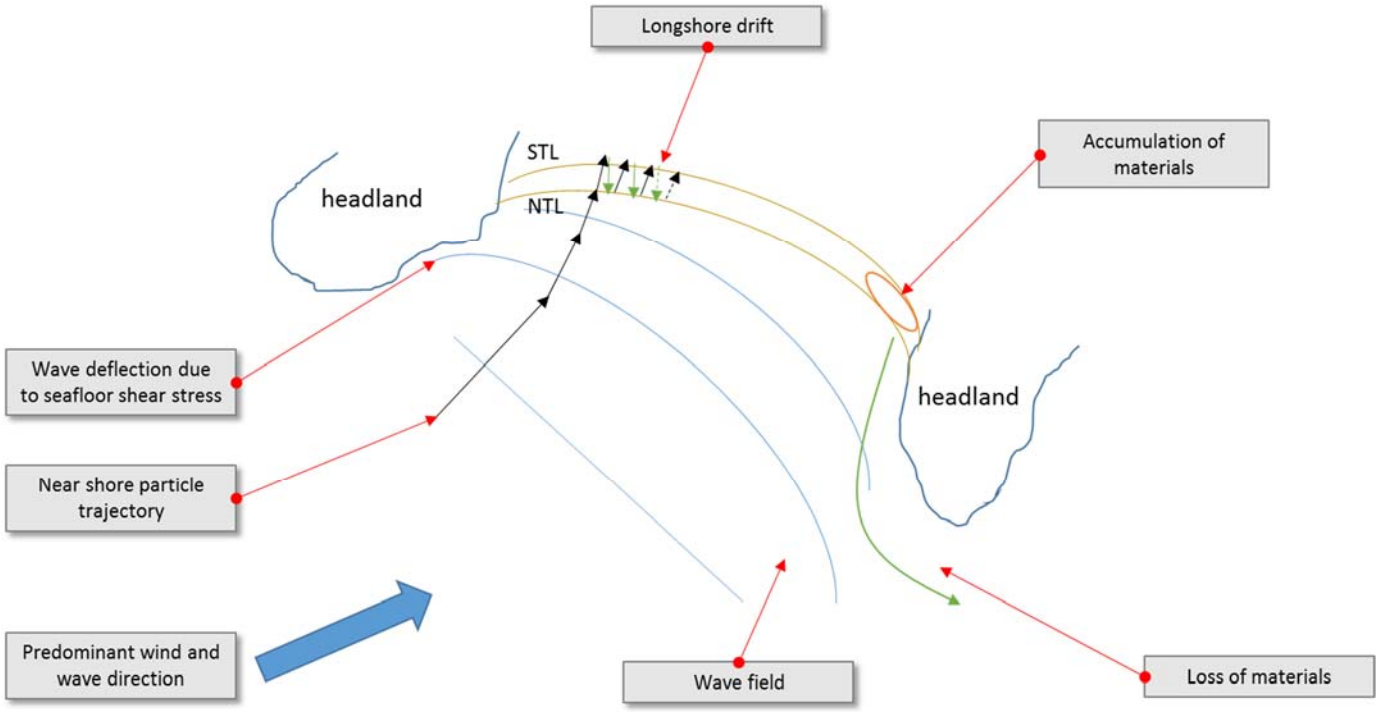

Figure 48: Conceptual framework for collection of materials on wave-dominated beaches with open shoreline aspects.

For restricted shoreline aspects, where the restriction may be due to closely spaced headlands through to submerged rocky outcrops, waves from a limited range of directions will be deflected into the embayment (Figure 49). These waves will transport materials on to the beach where longshore drift is less pronounced. Where rips occur they are not as likely to remove materials from the embayment and thus materials will be redeposited, leading to higher conservation and accumulation.

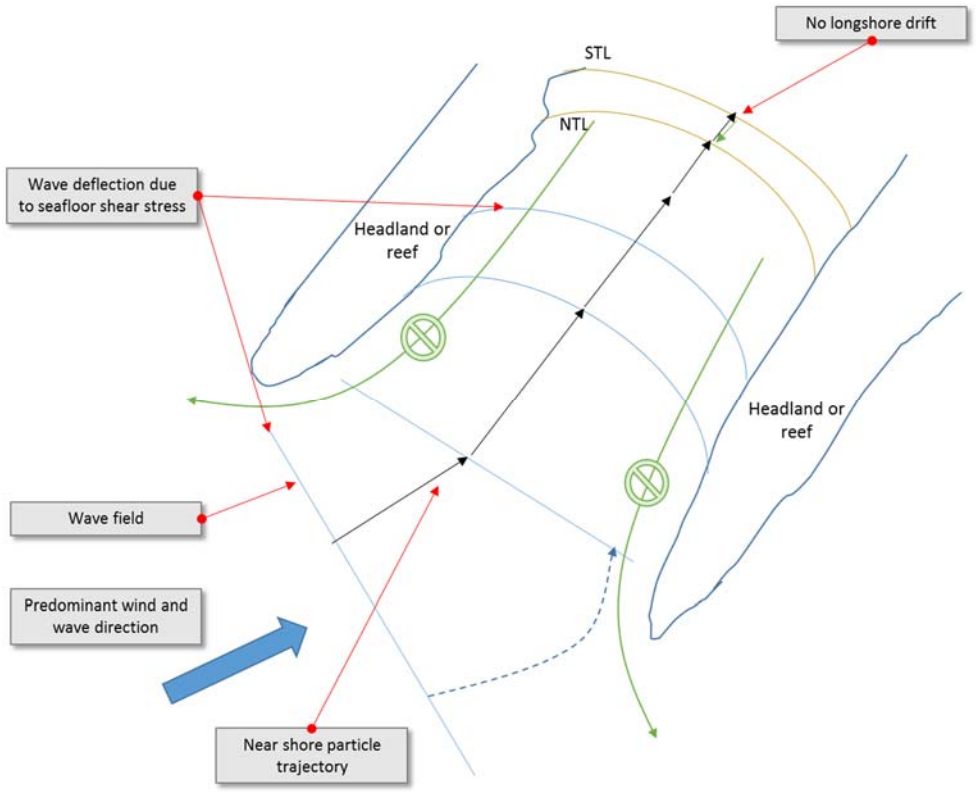

Figure 49: Conceptual framework for collection of materials on wave-dominated beaches with restricted shoreline aspects.

Distribution and occurrence of asphaltites and tarballs on the shoreline of South Australia

The geographic distribution of asphaltite and tarball/bitumen strandings along the South Australian coastline could lead to an appreciation of potential offshore origin points for the parent oils, as well as the processes give rise to their deposition on the shoreline.

In contemplating the distribution patterns described above, it is worth comparing them with those documented by previous workers in order to establish if the present study is representative of the amounts of materials coming ashore. Of particular relevance are the asphaltite and waxy bitumen studies of Padley (1995) and Edwards et al. (1998, 2016), as part of which quantitative beach surveys were conducted in 1990 and 1991 for a limited set of six beaches along the Limestone Coast. The numbers and total weights of specimens found by these workers are significantly higher than those encountered during this study (Figure 50).

This observation is intriguing and suggests that oil seepage in the source areas was higher prior to 1990 than at the present day. The samples collected during 1990 and 1991 were also less degraded (see section DEGRADATION OF OIL FAMILIES). There could be a number of reasons for these changes including, a reduction of seepage due to oil field production in Indonesia, reduced at-sea oil

tanker cleaning, or a particular geological event that led to a large release of hydrocarbons from the seafloor. Further interrogation of the respective data sets is required to attempt to understand the differences between these two studies.

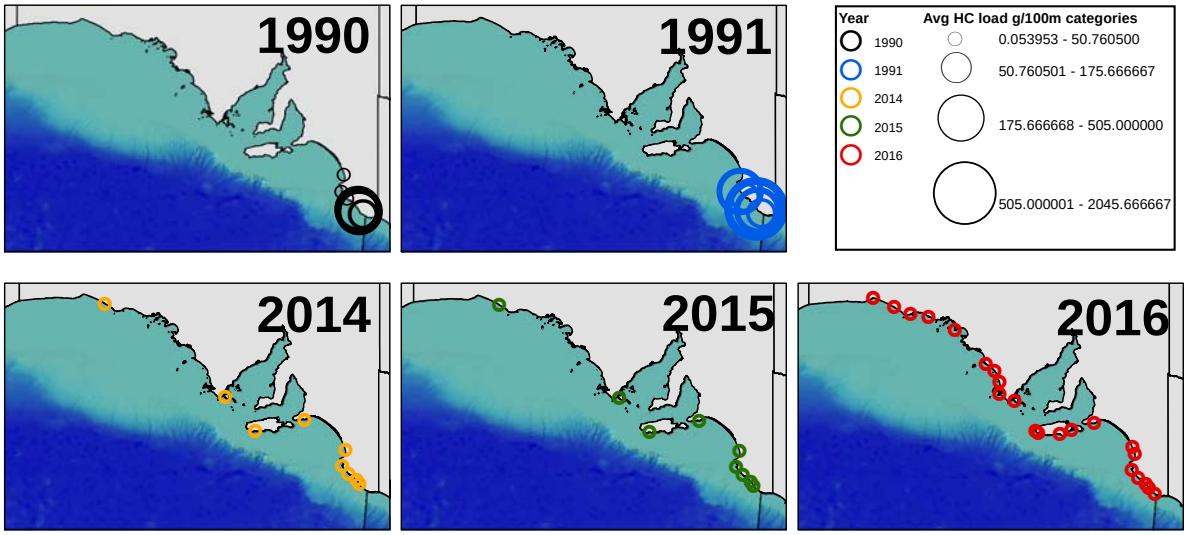

Figure 50: Hydrocarbon loadings along the South Australian coastline from coastline surveys between 1990 and 2016. Note that the 1990 and 1991 surveys shown were only for six selected beaches along the limestone coast.

The total number of asphaltite and tar-ball/waxy bitumen specimens collected in each year of this study are displayed geographically in Figure 51 and Figure 52. There are clear differences in their distributions: asphaltite strandings are more predominant on the Eyre Peninsula, whereas the tarball strandings are distributed across the region with the highest numbers of samples being encountered along the Limestone Coast close to the South Australian-Victorian border. The observed stranding distribution indicates that different processes are affecting the distribution of coastal bitumen across the region and could point to a local origin of the asphaltites further to the west than suggested by previous studies (Padley et al., 1993; Edwards et al., 1998; Boult et al., 2005; Hall et al., 2014), for example in the Duntroon and Ceduna sub-basins.

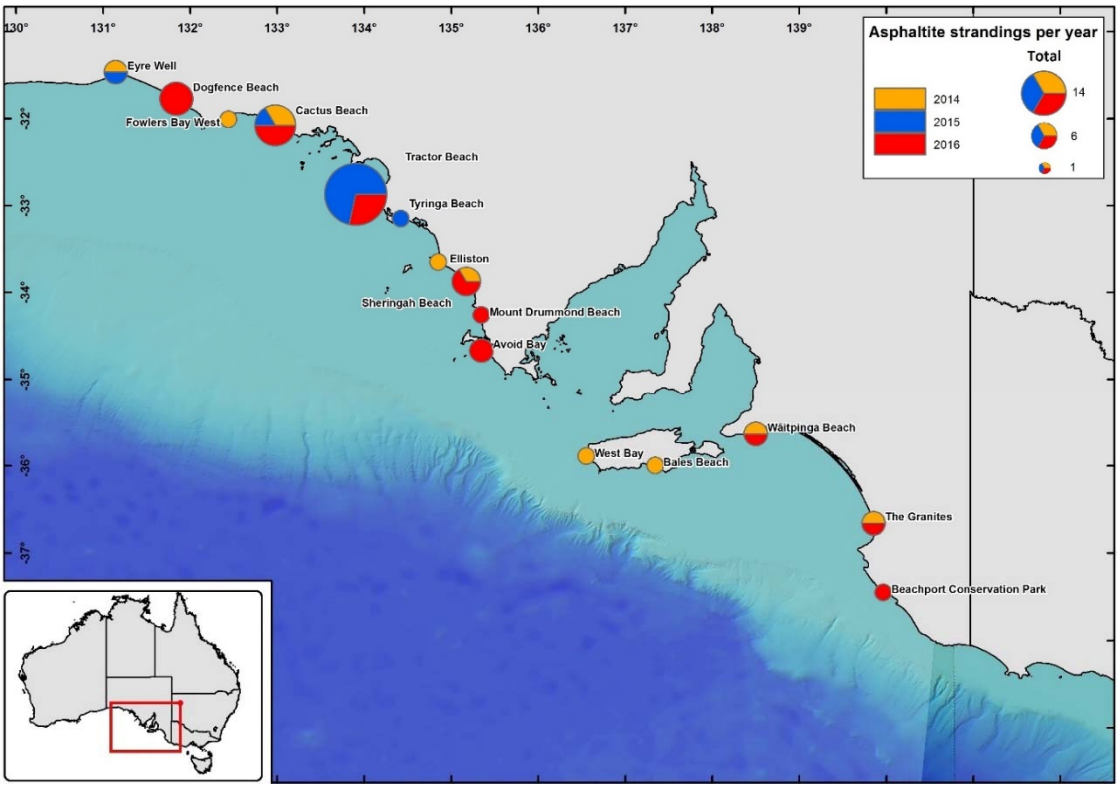

Figure 51: Total asphaltite strandings and distribution per year.

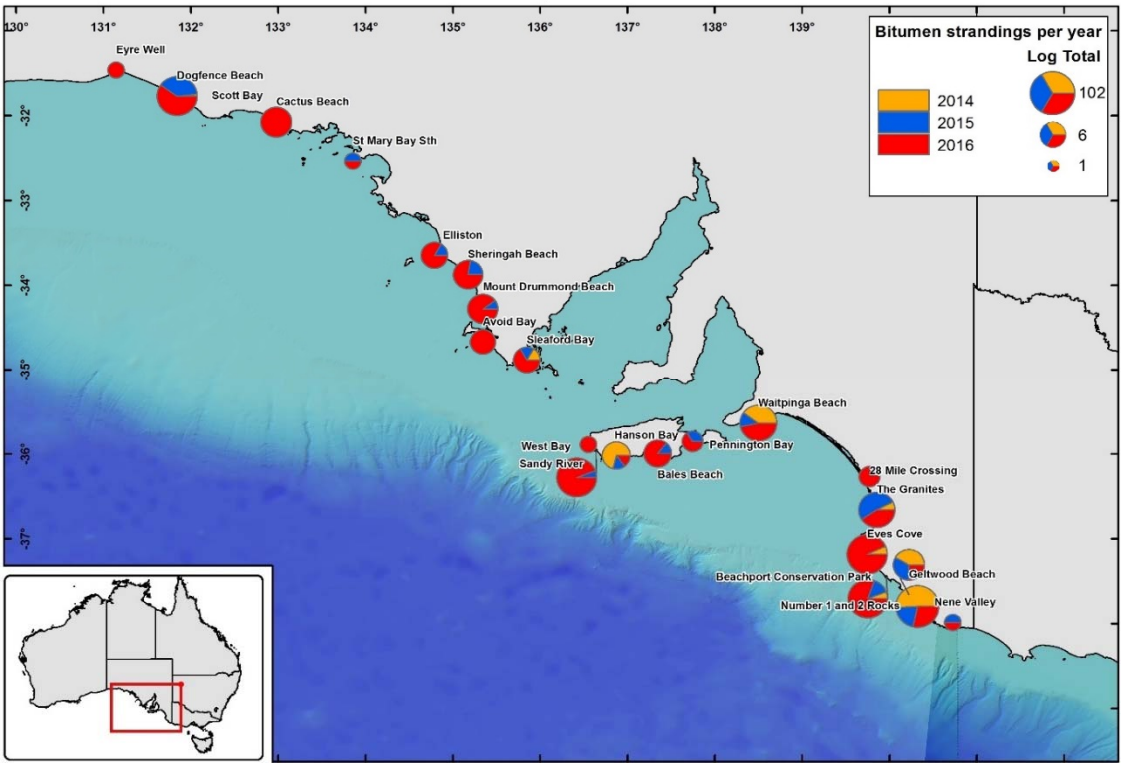

Figure 52: Total bitumen (tarball) strandings and distribution per year on a log scale.

When the stranding locations are identified according to oil family as determined by geochemical screening (see section OIL FAMILIES FROM BULK GEOCHEMICAL SCREENING) there are clear differences between the geographic distributions of the families (Figure 53). Bitumens of the Type III family (***no botryococcane, low wax)*** are distributed across much of the survey area, although weighted more toward the southern tip of Eyre Peninsula, Kangaroo Island and the Limestone Coast. Those of the Type IV family (***no botryococcane, high wax)*** have a very limited distribution due to the low numbers of samples shown to have this geochemical signature. Any interpretation of the geographic distribution of this oil family is therefore unlikely to be valid. Type II (***low botryococcane***) bitumens, with the exception of one sample, are found only on the Limestone Coast. The Type I (***high botryoccocane***) bitumens are by far the most abundant bitumen variety and it is predominantly found on Limestone Coast. With the exception of several samples assigned to the Type IV family, all the waxy bitumens have biomarker signatures indicative of an Indonesian origin. Their respective geographic distributions are consistent with their transport down the coast of Western Australian via the Leeuwin Current before being carried east on the coastal current and South Australian Current that traverse Australia's southern continental margin (Middleton & Bye, 2007; Edwards et al., 2016).

To explore the transport mechanisms for the asphaltites and tarballs these stranding locations were compared with the results of modelling aimed at determining the oceanographic processes that operate in the Great Australian Bight, with a view to locating potential seafloor origin points for the asphaltites and previously unknown bitumen waxy bitumens of non-Indonesian source affinity. These results are discussed in Part 4 Oceanography.

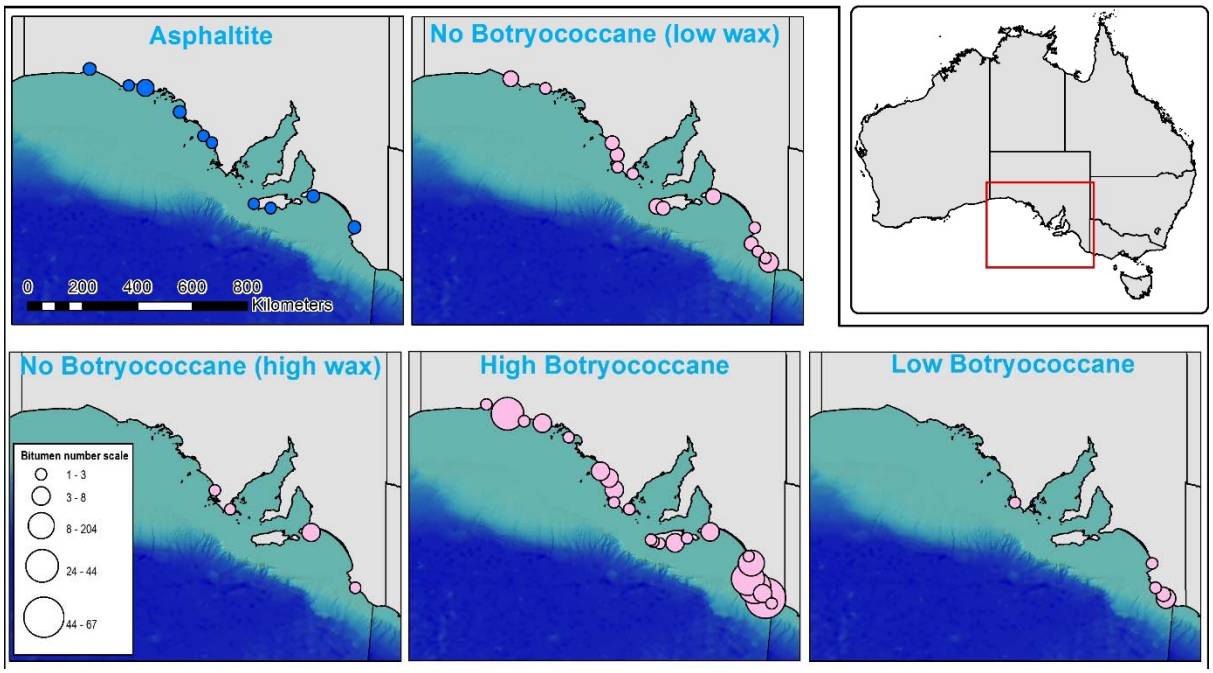

Figure 53: Distribution of asphaltite and main waxy bitumen families plotted to scale according to number of samples.

Summary and conclusions

The beach surveys for coastal bitumens conducted during the course of this project are the most comprehensive to date, both in their geographic extent and the data collected.

In summary:

- Thirty-one beaches were surveyed in November 2014, September 2015, and October 2016 extending from the Eyre Bird Observatory in Western Australia to Nene Valley near the South Australian-Victorian border. An average of 33.02 km of beaches were surveyed each year.
- The surveys collected data on beach morphology and character as well as other information such as anthropogenic contaminants (e.g. plastics and other debris).
- A total of 43 asphaltites, 2 greasy bitumens, 51 resins and ambers, 3 sooty bitumens and 464 waxy bitumens/tarballs were collected, which were further supplemented by donations of samples from members of the public.
- Of these materials 17% were collected in 2014, 20% in 2015 and 61% in 2016.
- Type I high botryococcane bitumens with strong geochemical affinities to Indonesian-sourced oils represented the most abundant sample type collected across all years.
- Strandings of asphaltite and bitumen typically occur on beaches with slopes of between 1 and 2 degrees. Analysis of the stranding position of an individual specimen may be indicative of the length of time spent on the beach and the winnowing effects of tides. No systematic variation of the pattern of stranding with beach width was observed.
- The predominant beach aspect for the combined sample totals of stranded asphaltite and waxy bitumens is to the southwest (by gross number). However, asphaltite strandings are most prevalent on beaches with a northwest aspect (data dominated by a high number of strandings on one beach). There are no evidence of a preferred stranding aspect for any individual tarball family.
- Detailed description of the example beaches has identified the dominant processes responsible for the collection and accumulation of materials on the beaches studied and led to the development of conceptual stranding models that provide an explanation for anomalously high sample numbers collected at Dogfence Beach and Number 1 & 2 Rocks.
- Differences between the quantities of materials stranded on the beaches in 1990–1991 and 2014–2016 cannot be explained, but may relate to a reduction in submarine oil seepage in Indonesia.
- Asphaltites have a different stranding pattern to tarballs/waxy bitumens suggesting different transport mechanisms and/or a different point of origin. The high abundance of waxy bitumens/tarballs with geochemical similarities to Indonesian-sourced oils along the Limestone Coast is consistent with the entrainment of these materials first in the southward Leeuwin Current and then in the eastward coastal and South Australian currents.
- Beach data and spatial stranding patterns along the coastline of South Australia will be used to interpret the outputs of oceanographic modelling conducted as part of this project.

Part 3 Geochemistry

INTRODUCTION

In order to determine the extent of weathering, and potential geochemical source, of the coastal bitumens collected from beaches in the study they were subjected to a suite of bulk and detailed geochemical analyses. The approach used a hierarchical sample analysis approach where progressively fewer samples were analysed using more detailed analysis. This approach was used in order to reduce unnecessary analysis. Both the geochemical methods used, representative data examples and interpretation of the geochemical data are presented in this section below.

ANALYTICAL RATIONALE AND METHODS

All analytical proceedures carried out on samples collected for Project 5.2 are summarised within Table 11. The aim of analyses carried out was to characterise all collected samples to allow the identification of a representative subset for detailed geochemical analyses for both oil family recognition and identification of features associated with biodegradation/water washing.

Table 11: Summary of analytical procedures. Any data still being collected (in progress) is not included or discussed in this report.

	Analyses	Samples analysed	Completion status
Physical documentation	Photograph	All samples	Complete
	Weigh		
	Measure along longest axis		
Bulk Geochemical analysis	Whole oil GC-MS	All samples	Complete
	Elemental analysis (% C,H,N,S)	All samples with sufficient material	Complete (*minor reruns*)
	Elemental analysis – isotope ratio mass spectrometry ($\delta^{13}C$, $\delta^{34}S$)	Representative subset	2014/15 = Complete *2016 In progress*
Detailed geochemical analysis	SIM GC-MS (biomarkers)	Representative subset selected	Complete
	GC-MS-MS (biomarkers)		Complete
	Saturates fraction EA-IRMS ($\delta^{13}C$)		*In progress*
	Aromatics fraction EA-IRMS ($\delta^{13}C$)		*In progress*
	CSIA of *n*-alkanes ($\delta^{13}C$, $\delta^{2}H$)		Complete
	High temperature GC-MS		Complete (*follow-up analysis proposed*)

SAMPLE PROCESSING

Physical documentation

All coastal bitumen samples collected across each of the three annual beach surveys were photographed with a Nikon D3100 DSLR with a macro lens, measured along their longest axis and weighed. All data from physical documentation may be found in APPENDIX 1: DATA MANAGEMENT.

Material falsely identified as bitumen and collected during beach surveys (e.g. black melted plastics or modern sedimentary peat samples) if identified prior to screening analyses, were not characterised.

Table 12: Tabulated summary of samples collected for each beach.

Beach_Name	Asphaltite	Greasy Bitumen	Resinite /Amber	Sooty Bitumen	Unknown	Waxy Bitumen	Other: charcoal, mudstone, peat, rock, seaweed and wood
28 Mile Crossing						3	0
Avoid Bay	3				3	101	0
Bales Beach	1		2		1	7	0
Beachport Conservation Park	1		1		1	51	0
Cactus Beach	6		6			11	0
Cape Bauer							1
Delisser Sandhills			2				1
Dogfence Beach	4	2	14		5	55	3
Elliston	1				1	6	0
Eves Cove				1		59	0
Eyre Well	2		5			2	0
Fowlers Bay West	1						0
Geltwood Beach				1		11	0
Greenly Beach	1				1	8	0
Hanson Bay			2		3	7	0
Mount Drummond Beach	1		2		2	10	0
Nene Valley					1	2	0
Number 1 and 2 Rocks			3		2	102	1
Pennington Bay						3	0
Point Peter			1		5		5
Sandy River			1		4	54	0
Scott Bay						1	0

Sheringah Beach	3	6	3	9	1
Sleaford Bay	1	4	3	17	0
St Mary Bay		1			0
St Mary Bay Sth				2	0
The Granites	2	1	1	27	0
Tractor Beach	14				0
Tyringa Beach	1		1		0
Waitpinga Beach	2		2	30	2
West Bay	1	1	1	1	0

Note: Table includes samples collected by Stuart Valladares in 2015 and 2016

See APPENDIX 1: DATA MANAGEMENT For the full table of samples collected

Bulk geochemical screening

All coastal bitumen samples were analysed by elemental analysis (EA) and whole-oil gas chromatograph mass spectrometry (GC-MS) to rapidly assess their bulk geochemistry for more detailed analysis.

Percentage of carbon, hydrogen, nitrogen and sulphur using elemental analysis

Elemental Analysis determines the percentage of carbon, hydrogen, nitrogen and sulphur for each sample.

All samples were analysed using a Perkin Elmer 2400 series II CHNS/O Elemental Analyzer in CHNS configuration at the University of Adelaide Biogeochemistry Lab Facilities. The combined combustion/reduction tube was packed using Perkin Elmer EA6000 and Perkin Elmer 'Hi-Purity' Copper with a reaction temperature was 975^{o}C. Results were calibrated to 3-4 mg of Perkin Elmer Organic Analytical Standard of Cystine (formula: $(SCH_2CH(NH_2)CO_2H)_2$) with known abundances of carbon (29.99 ± 0.3 %), hydrogen (5.09 ± 0.3 %), nitrogen (11.67 ± 0.3 %) and sulphur (26.69 ± 0.3 %). The accepted error range between standards for carbon, hydrogen and nitrogen was ± 0.3 %. Sulphur analysis resulted in a higher error, the accepted error for sulphur content was ± 0.5 %.

Preliminary oil family fingerprinting and degradation assessment using whole oil full scan gas chromatograph mass spectrometry

Whole oil gas chromatograph mass spectrometry (GC-MS) provides a rapid assessment of the compounds present in a hydrocarbon samples up to high molecular weight *n*-alkanes (C_{39}). This allows for preliminary geochemical screening based on the compounds present in high abundance (e.g. presence of high wax *n*-alkanes, ratio of pristane/phytane, etc). The technique also allows for an initial assessment of secondary processes which may have affected the sample, such as removal of low molecular weight compounds due to biodegradation.

Sample preparation

Each coastal bitumen collected was, sampled for ≥ 200 mg of material using a stainless steel scalpel and dissolved in 10 mL of a 93:7 mixture of dichloromethane (CH_2Cl_2) and methanol and stored in a 20 mL glass vial. Where possible, the interior and exterior (defined as the surficial 2 mm) were individually sampled. In cases where the bitumen samples were too small for interior/exterior sampling, a bulk sample was collected which includes both the interior and exterior. In instances where the entire sample was < 200 mg, the entire sample was dissolved. A 1 mL aliquot from each whole oil solution was then separated into a 2 mL chromatography vials for GC-MS analysis.

GC-MS method at University of Adelaide biogeochemistry facility

GC-MS analyses of the sample extracts for samples collected in 2014 and 2015 were performed on an Agilent 6890 gas chromatograph interfaced with a 5973N MSD (electron energy 70 eV) tuned using automatic setup parameters for each sequence. Chromatography was carried out on an Agilent HP-5MS fused silica column (30 m x 0.25 mm i.d. x 0.25µm film thickness), using either a split (50ml/min) or splitless injection modes conducted if split injection data showed low responses. The oven was programmed for an initial temperature of 50°C for 1 min, followed by heating at 8 °C/min to 300°C with a Helium carrier gas flow of 1 ml/min.

GC-MS analyses of the field season 3 sample extracts were performed on an Agilent 7890B gas chromatograph interfaced with a 5977B MSD (electron energy 70 eV) tuned using automatic setup parameters for each sequence. Chromatography was carried out on a J&W DB-5MS fused silica column (30 m x 0.25 mm i.d. x 0.25µm film thickness), using either a split (50ml/min) or splitless injection modes conducted if split injection data showed low responses. The oven was programmed for an initial temperature of 50°C for 1 min, followed by heating at 8 °C/min to 300°C with a Helium carrier gas flow of 1 ml/min.

The sample extracts were analysed by GC-MS in scan mode (Scan 45:500AMU at approx. 3 scans/sec) shown in Table 13. Retention times are listed are for split injections only.

Table 13: Targeted compounds in whole oil GC-MS geochemistry screening (split). Retention times are listed in minutes. Nd = not done (not present to identify or outside analytical range). Target ions for specific compounds were as follows: n-alkanes = 57; pristane = 57 + 183; phytane = 57 + 197; botryococcane = 57 + 294.

Compound (abbrev.)	2014 Retention Time	2015 Retention Time	2016 Retention Time
Octane (C8)	Nd	Nd	3.984
Nonane (C9)	Nd	Nd	5.618
Decane (C10)	7.510	7.460	7.509
Undecane (C11)	9.945	9.894	9.541
Dodecane (C12)	12.369	12.258	11.317
Tridecane (C13)	14.703	14.595	13.110
Tetradecane (C14)	16.923	16.818	14.844

Pentadecane (C15)	19.027	18.926	16.406
Hexadecane (C16)	21.020	20.924	17.919
Norpristane (Np)	21.907	21.801	18.576
Heptadecane (C17)	22.915	22.819	19.357
Pristane (Pr)	22.964	22.866	19.510
Octadecane (C18)	24.715	24.623	20.719
Phytane (Ph)	24.821	24.719	20.787
Nonadecane (C19)	26.430	26.341	22.020
Eicosane (C20)	28.068	27.981	23.256
Heneicosane (C21)	29.633	29.551	24.442
Docosane (C22)	31.134	31.054	25.575
Tricosane (C23)	32.572	32.496	26.663
Tetracosane (C24)	33.952	33.880	27.706
Pentacosane (C25)	35.281	35.212	28.713
Hexacosane (C26)	36.560	36.496	29.678
Heptacosane (C27)	37.793	37.730	30.609
Octacosane (C28)	38.987	38.926	31.509
Botryococcane (B)	39.478	39.429	31.924
Nonacosane (C29)	40.137	40.074	32.377
Triacontane (C30)	41.248	41.193	33.299
Hentriacontane (C31)	42.327	42.275	34.347
Dotriacontane (C32)	43.413	43.356	35.563
Tritriacontane (C33)	44.643	44.661	37.013
Tetratriacontane (C34)	46.086	46.106	38.745
Pentatriacontane (C35)	47.806	47.829	40.833
Hexatriacontane (C36)	49.809	49.907	43.363
Heptatriacontane (C37)	52.296	52.399	46.483
Octatriacontane (C38)	55.237	55.426	Nd
Nonatriacontane (C39)	58.885	59.132	Nd

Carbon and sulphur isotopic compositions using elemental analysis - isotope ratio mass spectrometry (EA-IRMS)

Sample preparation

Elemental Analysis - Isotope Ratio Mass Spectrometry (EA-IRMS) was used to determine the bulk carbon and sulphur isotopic composition of selected samples. Subsamples from collected coastal bitumen samples were collected using a stainless steel scalpel cleaned with hexane to prevent cross-contamination. These sub-samples were placed in 5x9 mm tin cups and analysed by the University of Adelaide Isotope Ratio Mass Spectrometry Facility.

EA-IRMS method at University of Adelaide biogeochemistry facility

Carbon and sulphur isotope data was collected using a Eurovector EuroEA Elemental Analyzer modified with a valco valve to allow separation of combusted SO_2 from CO_2 and N2.

Carbon isotope results were calibrated to 1mg of in-house standards of glycine (-31.2 ‰), glutamic acid (-16.76 ‰) and triphenylamine (-29.2 ‰). Acceptable maximum error range for $\delta^{13}C$ values was ± 0.1 ‰.

Sulphur isotope results were calibrated to two in-house standards (S2 and S3) of silver sulphide (Ag_2S) with $\delta^{34}S$ values of +22.7 ‰ and -32.3 ‰ respectively. Due to the range in sulphur content (< 0.2 % to 4 %) across the different varieties of coastal bitumen, the weight of standards varied between 2-4 mg. The accepted maximum error range for $\delta^{34}S$ values was ± 0.38 ‰, though this was largely restricted to samples with low (<1 %) sulphur content. Samples with higher sulphur content typically resulted in a lower error with a standard deviation of ± 0.16.

Isotope results are presented in the conventional delta (δ) notation, which presents the stable isotopic ratio of the sample relative to that of a known international standard. For carbon isotopes ($\delta^{13}C$), the international standard for delta notation is the Vienna Peedee Belemnite (VPDB) and is calculated using the following equation:

$$\delta^{13}\mathrm{C} = \left(\frac{\left(\frac{^{13}C}{^{12}C}\right)_{sample}}{\left(\frac{^{13}C}{^{12}C}\right)_{VPDB}} - 1 \right) \times 1000\ ‰$$

For sulphur isotopes ($\delta^{34}S$) the international standard for delta notation is the Canyon Diablo Troilite (CDT) and is calculated using the comparable equation:

$$\delta^{34}\mathrm{S} = \left(\frac{\left(\frac{^{34}S}{^{32}S}\right)_{sample}}{\left(\frac{^{34}S}{^{32}S}\right)_{CDT}} - 1 \right) \times 1000\ ‰$$

Detailed geochemical analyses

Specific samples from each whole oil family determined from initial screening were selected for further detailed analysis. The subset selection included samples from each oil family defined using the whole oil classification scheme in a variety of different stages of degradation in order to determine results from the freshest material in addition to identifying the effects of weathering on key geochemical parameters.

Fractionation by liquid chromatography

Compounds commonly used to interpret source palaeoenvironmental conditions, thermal maturity and biodegradation are often present in relatively low abundance in comparison to other hydrocarbons (e.g. *n*-alkanes). To analyse these components, hydrocarbons are separated into their saturated, aromatic and polar fractions and concentrated prior to analysis.

Of interest here are the saturated and aromatic fractions separated using the elution method described by Bastow et al., (2007) and summarised below.

Disposable pasteur pipette columns were prepared with 10 mm of packed quartz wool followed by 50 mm (ca. 0.6 g) of silica gel for a 1.8 mL elution. Separation of saturated, aromatic and polar fractions requires the silica gel to be activated by heating at ≥ 110ºC for at least 8 hours. Prior to sample separation, three bed volumes (0.8 mL) of analytical grade *n*-pentane was passed through each column.

A 2 mL aliquot from the previously prepared whole oil solutions was dried to remove the solution of dichloromethane and methanol. This bitumen was then dissolved in a minimum amount of n-pentane, ensuring dissolution of saturated, aromatic and polar compounds while leaving a residue of the insoluble asphaltene fraction. This concentrated sample solution was then added to the top of the prepared separation column to produce a concentrated band (Figure 54). Each prepared column is eluted with three different solvent mixtures, the separation and collection of the saturated, aromatic and polar fractions. Separation of saturated hydrocarbons was achieved using a solution of *n*-pentane. Where under gravity three small volumes of n-pentane (0.1 mL) were passed through the column, followed by single volume of 0.6 mL and 0.9 mL respectively. Saturated fractions were eluted into 2 mL vials.

Separation of aromatic hydrocarbons was achieved using a 7:3 ratio mixture of n-pentane and dichloromethane following elution of the saturated hydrocarbons fraction. Three volumes of 0.1 mL elutions of the n-pentane/dichloromethane mixture were passed through the column under gravity, followed by single elutions of 0.6 mL and 0.9 mL respectively. Aromatic fractions were stored in 2 mL amber glass vials to ensure minimal degradation to the aromatic fraction from ultraviolet light.

For reference, following removal of the aromatic fraction the polar compounds may also be separated using a 1:1 mixture of dichloromethane and methanol using the same elution steps outlined above. However, the polar fraction was not analysed.

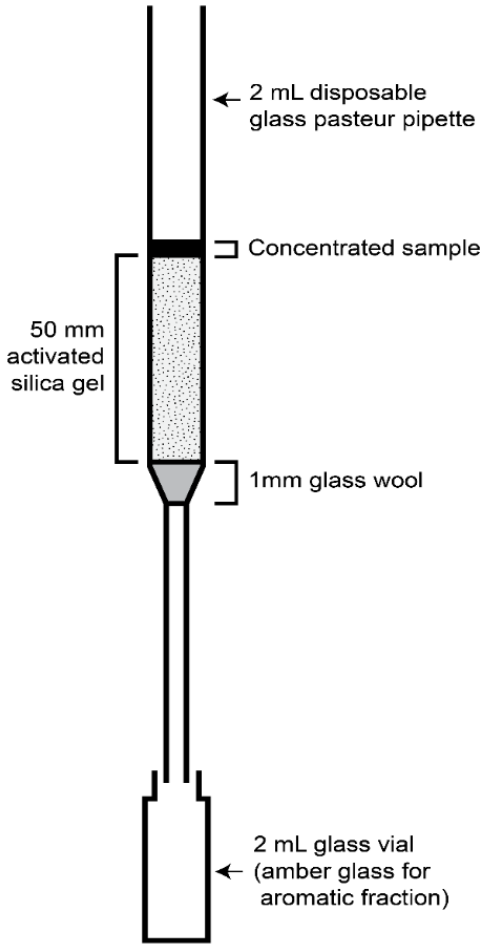

Figure 54: Pasteur pipette configuration for separation of saturated, aromatic and polar fractions.

Molecular sieve fractionation of branched and cyclic saturated hydrocarbons

Biomarker analysis was affected by high content of *n*-alkanes in the saturate fractions for most of the waxy bitumen samples so that branched/cyclic alkanes to be separated from n-alkanes by molecular sieve methodology. Molecular sieve (A5, 60-80 mesh) was baked in a furnace at 450ºC overnight prior to use. Around 0.2 g baked molecular sieve was weighed into a 4 mL vial. 1 mg of saturate fraction dissolved in a minimum volume of cyclohexane was then quickly transferred into this 4 mL vial which was then topped up to 4 mL with cyclohexane. The 4 mL vial was then put into an 80ºC oven overnight. *n*-Alkanes was absorbed on the molecular sieves and branched/cyclic alkanes was left in the cyclohexane. The branched/cyclic alkanes in cyclohexane in the 4 mL vial were transferred into another 2 mL vial after the 4 mL vial was taken out from the oven. The molecular sieve was then washed with cyclohexane for three times which was then combined into the 2 mL vial and volume reduced to the right concentration for GC-MS analysis.

Saturated fraction biomarker analysis using selected ion monitoring (SIM) gas chromatograph mass spectrometry

Analysis of branch/cyclic alkanes

GC-MS analyses of the saturate or branched/cyclic fractions were performed on an Agilent 7890A gas chromatograph interfaced with a 5975C MSD (electron energy 70 eV) tuned using automatic setup parameters on the day of the analysis. Chromatography was carried out on a J&W DB-5MS fused silica column (60 m x 0.25 mm i.d. x 0.25µm film thickness), using a split/splitless injector technique. The oven was programmed from an initial temperature of 40°C for 2 min., followed by heating at 20 °C/min to 200°C and then a second heating ramp at 2°C/min to 310°C with a Helium carrier gas flow of 1.5 mL/min.

The saturate or branched/cyclic fractions were analysed using a single ion monitoring (SIM) programme as shown below:

- *m/z* 177, 183, 191, 205, 217, 218, 231, 253, 259.

For oil family classification the primary components assessed were steranes/diasteranes (m/z 217, 218, 259) and terpanes (m/z 191). The compounds targeted in these mass fragments are summarised in Table 14 and Table 15.

Table 14: Target compounds in m/z 217, 218, 259 (steranes). Note retention times for biomarkers varied by ± 1 minute required manual integration for all samples.

Compound	Abbreviation	Ion (m/z)	RT (± 1 min)
Pregnane	S20	217	32
Homopregnane	S21	217	36
C27 βα 20S diacholestane	27DbaS	217	47
C27 βα 20R diacholestane	27DbaR	217	48
C27 αβ 20S diacholestane	27DabS	217	48
C27 αβ 20R diacholestane	27DabR	217	49
C28 βα 20S diasterane a	28DbaSA	217	49
C28 βα 20S diasterane b	28DbaSB	217	50
C28 βα 20R diasterane a	28DbaRA	217	51
C28 βα 20R diasterane b	28DbaRB	217	51
C27 αα 20S cholestane	27aaS	217	52
C27 ββ 20R cholestane	27bbR	217	52
C27 ββ 20S cholestane	27bbS	217	52
C27 αα 20R cholestane	27aaR	217	53
C28 αα 20S ergostane	28aaS	217	55
C28 ββ 20R ergostane	28bbR	217	55

C28 ββ 20S ergostane	28bbS	217	56
C28 αα 20R ergostane	28aaR	217	56
C29 αα 20S stigmastane	29aaS	217	57
C29 ββ 20R stigmastane	29bbR	217	58
C29 ββ 20S stigmastane	29bbS	217	58
C29 αα 20R stigmastane	29aaR	217	59
C30 αα 20S propylcholestane	30aaS	217	59
C30 ββ 20R propylcholestane	30bbR	217	60
C30 ββ 20S propylcholestane	30bbS	217	60
C30 αα 20R propylcholestane	30aaR	217	61
C27 ββ 20R cholestane	27bbR	218	52
C27 ββ 20S cholestane	27bbS	218	52
C28 ββ 20R ergostane	28bbR	218	55
C28 ββ 20S ergostane	28bbS	218	56
C29 ββ 20R stigmastane	29bbR	218	58
C29 ββ 20S stigmastane	29bbS	218	58
C27 βα 20S diacholestane	27DbaS	259	47
C27 βα 20R diacholestane	27DbaR	259	48
C28 βα 20S diaergostane a	28DbaSA	259	49
C28 βα 20S diaergostane b	28DbaSB	259	50
C28 βα 20R diaergostane a	28DbaRA	259	51
C28 βα 20R diaergostane b	28DbaRB	259	51
C29 βα 20S diastigmastane	29DbaS	259	52
C29 βα 20R diastigmastane	29DbaR	259	53
Tetracyclic polyprenoid Ta	30TPPa	259	61
Tetracyclic polyprenoid Tb	30TPPb	259	61

Exact retention times specific to each sample are recorded in Appendix 7.

Table 15: Target compounds in m/z 191 (terpanes). Note that retention times for biomarkers varied by ± 1 minute.

COMPOUND	ABBREVIATION	ION (M/Z)	RT (± 1 MIN)
C19 tricyclic diterpane	C19t	191	24
C20 tricyclic diterpane	C20t	191	27
C21 tricyclic diterpane	C21t	191	29
C22 tricyclic terpane	C22t	191	31
C23 tricyclic terpane	C23t	191	35
C24 tricyclic terpane	C24t	191	36

C25 tricyclic terpane (S)	C25tS	191	40
C25 tricyclic terpane (R)	C25tR	191	40
C24 tetracyclic terpane (TET)	C24T	191	43
C26 tricyclic terpane (S)	C26tS	191	43
C26 tricyclic terpane (R)	C26tR	191	43
C28 extended tricyclic terpane (S)	C28tS	191	50
C28 extended tricyclic terpane (R)	C28tR	191	50
C29 extended tricyclic terpane (S)	C29tS	191	52
C29 extended tricyclic terpane (R)	C29tR	191	52
C30 extended tricyclic terpane (S)	C30tS	191	56
C30 extended tricyclic terpane (R)	C30tR	191	56
Ts 18a(H)-trisnorhopane	Ts	191	54
Tm 17α(H)-trisnorhopane	Tm	191	56
C28 17α18α21β(H)-bisnorhopane	C28BNH	191	58
C29 Nor-25-hopane	Nor25H	191	59
C29 Tm 17α(H)21β(H)-norhopane	C29H	191	60
C29 Ts 18α(H)-norneohopane	C29Ts	191	60
C30 17α(H)-diahopane	C30DiaH	191	60
C29 normoretane	Normor	191	61
α-oleanane	a-Ole	191	62
β-oleanane	b-Ole	191	62
C30 17α(H)-hopane	C30H	191	62
17α(H)-30-nor-29-homohopane	C30Ts	191	63
C30 moretane	Mor	191	64
C31 22S 17α(H) homohopane	C31HS	191	65
C31 22R 17α(H) homohopane	C31HR	191	66
gammacerane	Gam	191	67
C32 22S 17α(H) bishomohopane	C32HS	191	68
C32 22R 17α(H) bishomohopane	C32HR	191	68
C33 22S 17α(H) trishomohopane	C33HS	191	71
C33 22R 17α(H) trishomohopane	C33HR	191	72
C34 22S 17α(H) extended hopane	C34HS	191	75
C34 22R 17α(H) extended hopane	C34HR	191	77
C35 22S 17α(H) extended hopane	C35HS	191	80
C35 22R 17α(H) extended hopane	C35HR	191	82

Exact retention times specific to each sample are recorded in Appendix 7.

Saturated fraction biomarker analysis using gas chromatography coupled to tandem mass spectrometry (gc-ms-ms) with cold electron ionisation

GC-MS-MS analyses of the saturate or branched/cyclic fractions were performed on a Perkin Elmer 680 Clarus gas chromatograph interfaced with a Perkin Elmer iQT Quadropole Time of Flight (QToF) mass spectrometer fitted with a Cold-EI source tuned using automatic setup parameters for each sequence. Chromatography was carried out on a J&W DB-5MS fused silica column (60 m x 0.25 mm i.d. x 0.25µm film thickness), using a split/splitless injector operating in splitless mode. The oven was programmed from an initial temperature of 50°C for 1 min., followed by heating at 12 °C/min to 180°C and then a second heating ramp at 4°C/min to 310°C with a Helium carrier gas flow of 2mL/min. The saturate or branched/cyclic fractions were analysed using a metastable reaction monitoring (MRM) programme shown in Table 16.

Aromatic fraction biomarker analysis using gas chromatography mass spectrometry (gc--ms)

GC-MS analyses of the aromatic fractions were performed on a Perkin Elmer 680 Clarus gas chromatograph interfaced with a Perkin Elmer iQT Quadropole Time of Flight (QToF) mass spectrometer fitted with a Cold-EI source, tuned using automatic setup parameters for each sequence. Chromatography was carried out on a Perkin Elmer PE-5MS fused silica column (30 m x 0.25 mm i.d. x 0.25µm film thickness), using a splitless injection technique. The oven was programmed for an initial temperature of 50°C for 1 min., followed by heating at 8 °C/min to 300°C with a Helium carrier gas flow of 2mL/min.

The aromatic fractions were analysed using a ToF ion collection programme (Scan 45:450AMU at approx. 5 counts/sec).

Table 16: Summary of target compounds for MRM analysis. TT = tricyclic terpanes; Tet = tetracyclic terpanes. Channel ranges for each compound are given.

Channel	Parent Ion	Daughter Ion	Channel Range	
C19 TT	262	191	17.5	27.5
C20 TT	276	191	19.5	29.5
C21 TT	290	191	21.5	31.5
C22 TT	304	191	24.0	34.0
C23 TT	318	191	26.5	36.5
C24 TT	332	191	28.0	38.0
C25 TT	346	191	31.0	41.0
C26 TT	360	191	33.5	43.5
C27 TT	374	191	38.0	48.0
C28 TT	388	191	40.0	50.0
C29 TT	402	191	41.0	51.0

C30 TT	416	191	44.0	54.0
C24 Tet	330	191	33.5	43.5
C25 Tet	344	191	36.0	46.0
Hopanes	370	191	43.0	53.0
Hopanes	384	191	44.0	56.0
Hopanes	398	191	47.0	57.0
Hopanes	412	191	49.0	59.0
Hopanes	426	191	51.5	61.5
Hopanes	440	191	53.5	63.5
Hopanes	454	191	56.0	66.0
Hopanes	468	191	58.5	68.5
Hopanes	482	191	62.0	70.0
C26 Steranes	358	217	34.0	46.0
C27 Steranes	372	217	39.0	51.0
C28 Steranes	386	217	42.0	54.0
C29 Steranes	400	217	45.0	57.0
C30 Steranes	414	217	48.0	60.0
Methyl Steranes	414	231 to 238	47.0	61.0
Bicadinanes	412	412	40.0	60.0
Bicadinanes	412	369	40.0	60.0
Bicadinanes	426	383	40.0	60.0

For exact retention times within these channels see results for specific samples in Appendix 7.

Carbon isotopic composition of specific hydrocarbons using compound specific isotope analysis (CSIA)

Compound specific isotope analysis (CSIA) provides an individual isotopic composition for each specified compound within a sample. Previously Hall et al., (2014) proposed that variation in the carbon isotopic composition of *n*-alkanes between the exterior and interior of asphaltite strandings may be used to assess the extent of biodegradation and water washing.

Sample preparation

Molecular sieve methodology was selected for separating *n*-alkanes from branched/cyclic alkanes in the saturate fractions of the asphaltite and waxy bitumen samples. Molecular sieve (A5 60-80 mesh) was baked in a furnace at 450ºC overnight prior to use. The baked molecular sieve (~1.5g) was weighed into a 20 mL vial. The saturate fraction (~10 mg) dissolved in a minimum volume of cyclohexane was quickly transferred into this 20 mL vial which was then topped up to 10 mL with cyclohexane. The 20 mL vial was put in an 80ºC oven overnight. The *n*-Alkanes were sorbed into the molecular sieves and the branched/cyclic alkanes remained in the cyclohexane. The excessive cyclohexane in the vial was removed after the 20 mL vial was taken out from the oven. The molecular sieves were then washed with cyclohexane three times to remove any possible

branched/cyclic alkanes on the sieves. The molecular sieve with sorbed *n*-alkanes was left in fume cupboard to dry and then transferred into a 20 mL Teflon tube. HF was added into the Teflon tube dropwise to digest the molecular sieve until the molecular sieve was totally dissolved. Pentane was then added into the Teflon tube to extract the n-alkanes. Pentane extraction was repeated three times to maximise the extraction efficiency. The extracted *n*-alkanes were concentrated into a 2 mL vial to near dryness (using a gentle stream of nitrogen) and were then sent to the Davis Isotope laboratory in the University of California for CSIA analysis.

CSIA method in Davis Isotope Laboratory

The carbon isotopic compositions of *n*-alkanes of asphaltite and waxy bitumen samples were measured by GC-C-IRMS (gas chromatography/combustion/isotope-ratio mass spectrometry). The GC-C-IRMS system consisted of a GC unit (6890N, Agilent Technologies, USA) connected to a GC-C/TC III combustion device coupled via open split to a Thermo MAT 253 mass spectrometer. The analytes of the GC effluent stream were oxidised to CO2 in the combustion furnace held at 950°C on a CuO/NiO/Pt catalyst. CO2 was transferred on-line to the mass spectrometer to determine carbon isotope ratios. 1 µL of n-alkane fraction was injected to the split/splitless inlet system in a splitless mode (1min.). The injector was held at a temperature of 290°C. The n-alkanes were separated on a fused silica capillary column (BP-5 (SGE), 30 m x 0.25 mm ID, 0.25 mm film). The GC was held at 50°C for 2min., followed by heating at 25°C/min to 120°C and then a second heating ramp at 5°C/min to 310°C and held for 8 min. All samples were measured with a standard deviation of replicate measurements of individual *n*-alkanes from *n*-alkane reference materials (IU A6 and B3) of ≤1 ‰. Provisional $\delta^{13}C$ measurements are made by comparison to an internal standard (C12:0) of known $\delta^{13}C$ composition. Two mixtures of pure n-alkanes of calibrated δ13C measurement (Indiana University, Mixtures A6 and B3), were co-analysed with samples. One mixture was used for isotopic calibration of δ13C measurements (B3), while the other was not involved in calibration and served as the primary quality assessment material (A6).

The hydrogen isotopic compositions of *n*-alkanes of asphaltite and waxy bitumen samples were measured by GC-C-IRMS (gas chromatography/combustion/isotope-ratio mass spectrometry). The GC-C-IRMS system consisted of a GC unit (6890N, Agilent Technologies, USA) connected to a GC-TC pyrolysis interface coupled via open split to a Thermo MAT 253 mass spectrometer. After passing through the GC, hydrocarbons were reduced to H_2 and elemental carbon in the pyrolysis reactor held at 1450°C. H_2 was transferred on-line to the mass spectrometer to determine hydrogen isotope ratios. 1 µL of *n*-alkanes were injected to the split/splitless inlet system in a splitless mode (1 min.). The injector was held at a temperature of 290°C. The *n*-alkanes were separated on a fused silica capillary column (BP-5 (SGE), 30 m x 0.25 mm ID, 0.25 mm film). The GC was held at 50°C for 2 min., followed by heating at 25°C/min to 120°C and then a second heating ramp at 5°C/min to 310°C and held for 8 min. All samples were measured with a standard deviation of replicate measurements of individual *n*-alkanes from *n*-alkane reference materials (IU A6 and B3) of ≤1 ‰. Provisional $\delta^{2}H$ measurements were made by comparison to an internal standard (C12:0) of known $\delta^{2}H$ composition. Two mixtures of *n*-alkanes of calibrated $\delta^{2}H$ measurement (Indiana University, Mixtures A6 and B3), were co-analysed with samples. One mixture was used for isotopic calibration of $\delta^{2}H$ measurements (B3), while the other was not involved in calibration and served as the primary quality assessment material (A6).

OIL FAMILIES FROM BULK GEOCHEMICAL SCREENING

Classification of Coastal Bitumen

Due to the high number of samples collected, sample classification took a tiered approach. All potential coastal bitumen samples were assessed visually upon identification on the beach, then bitumen samples underwent bulk geochemical screening to identify representative samples for source-specific biomarker analysis to interpret characteristics of the parent petroleum system and therefore likely provenance.

Visual Classification of Stranded Materials

Physical characteristics of stranded materials may be used to assign a preliminary classification to collected specimens upon collection in the field. If samples could not be easily identified they were classified as 'Unknown' samples to be characterised geochemically.

Asphaltites

Asphaltites are the most visually distinct variety of coastal bitumen encountered along the South Australian coastline (Figure 55). Often larger than waxy bitumen, asphaltites are most commonly flattened, ovoid bitumen (e.g. Figure 55A-C) however in rare instances larger strandings prove an exception to this observation (e.g. Figure 55E). Asphaltites also have a strong petroliferous odour and contain deep shrinkage cracks throughout its outer surface. Most asphaltites are brittle, and when sampled for geochemical analysis will break open to reveal a diagnostic conchoidal fracture (Figure 55D). This occurs in all but the freshest collected asphaltites, which still contain a soft and pliable interior which does not fracture. However, the exterior of these fresh samples is often still brittle and cracked, resulting in small conchoidal fractures visible on the outer surface (e.g. Figure 55E).

Waxy Bitumen

Waxy bitumens are the most common variety of coastal bitumen encountered along the South Australian coastline. These bitumens are usually semi-rounded tarballs between 1 to 5 cm in diameter (Figure 56), although rare examples may be up to ca. 10 cm in diameter. These bitumens are usually semi-solid, becoming increasingly brittle when heavily weathered. Unlike the asphaltites, when brittle waxy bitumen will not break with a conchoidal fracture. Many waxy bitumen show surficial browning of the increasingly brittle exterior, although the interior remains black (Figure 56C-D). Whilst this browning does demonstrate a degree of weathering, other examples of similarly degraded waxy bitumen have also remained entirely black. We tentatively suggest that the browning is related to a higher degree of weathering via photo-oxidation compared to other examples where degradation may be attributed to higher degrees of biodegradation and water washing.

Whilst there are numerous varieties of waxy bitumen which may be identified based on their geochemistry (discussed below), there are no clearly diagnostic visual features by which they can be separated.

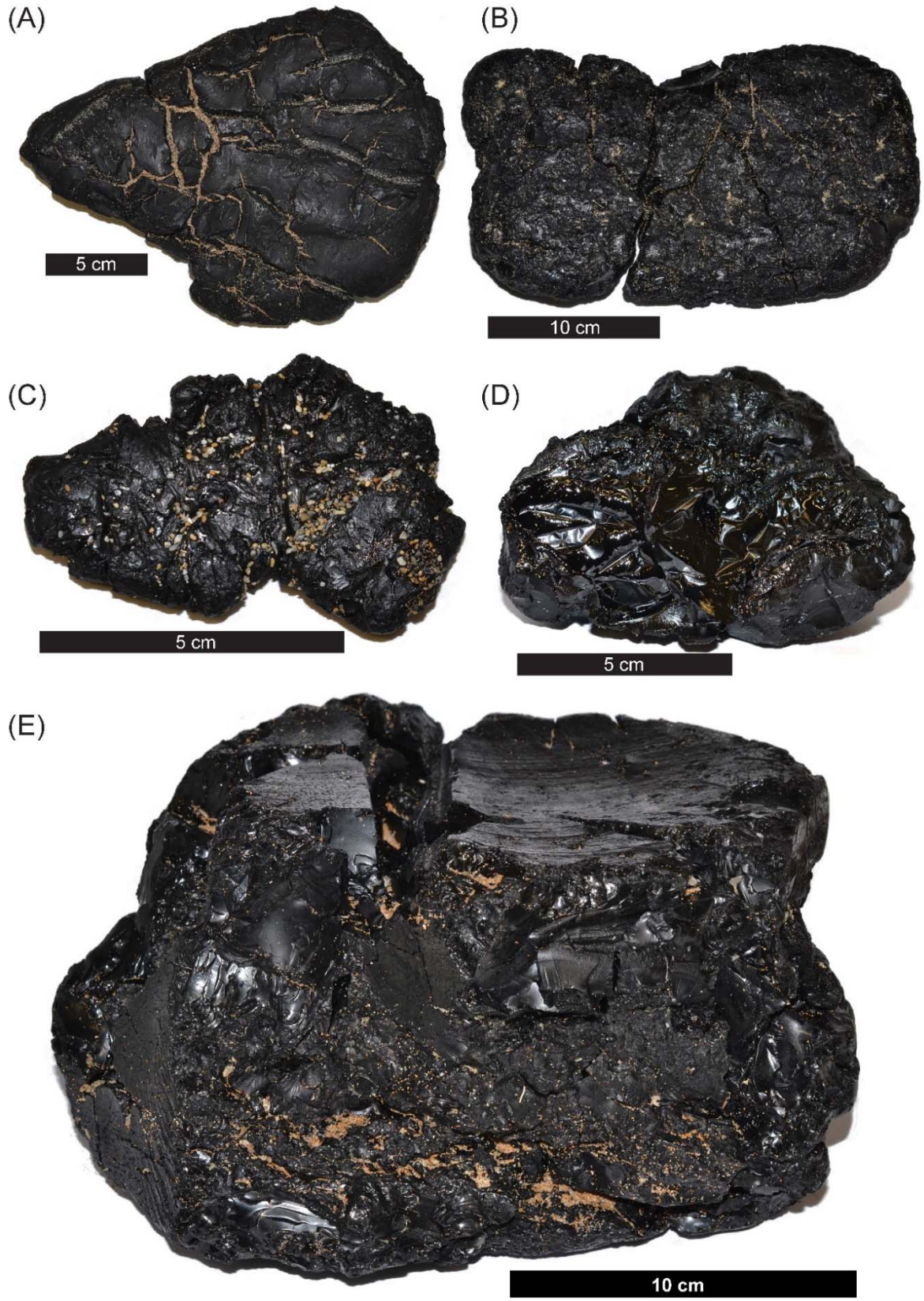

Figure 55: Examples of asphaltite. (A) Sample W13/007507. (B) Sample W13/007672. (C) Sample W13/007473. (D) Sample W13/007742 opened in half, demonstrating the characteristic conchoidal fracture exhibited by the asphaltites. (E) Sample W13/007976, the largest and freshest asphaltite collected (3.3 kg with a soft interior).

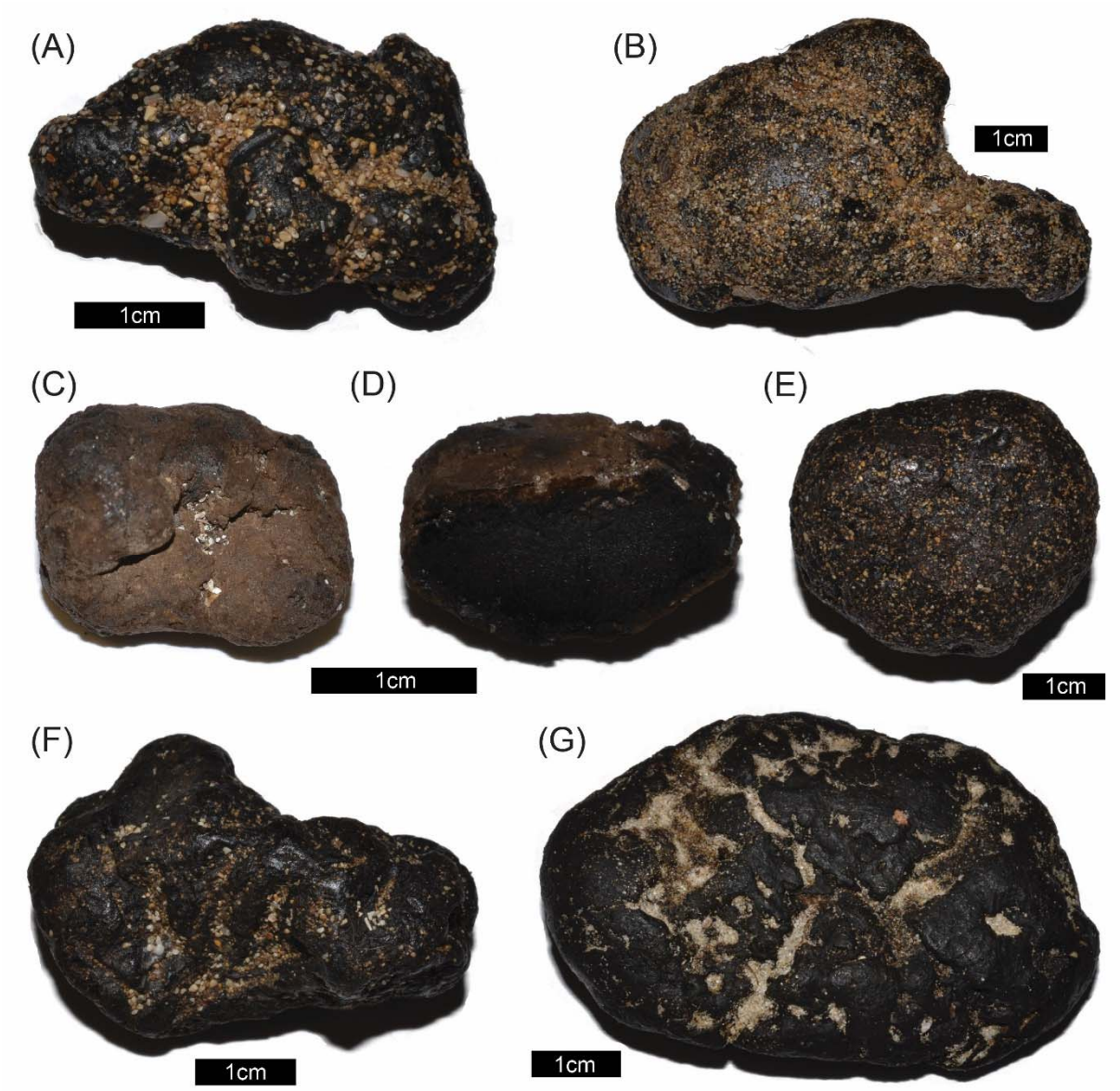

Figure 56: Examples of waxy bitumen. (A) Sample W13/007700. (B) Sample W13/007697. (C) Sample W13/007521. (D) Sample W13/007521 cut in half to reveal black interior. (E) Sample W13/007680. (F) W13/007683. (G) Sample W13/007601.

Coastal Resin/Amber

Fragments of resin and resinite (fossilised resin) are also known to strand along the South Australian coastline (Murray et al., 1994a, Padley., 1995). Resinites are visually distinctive, largely black in colour with brown/golden highlighted areas (Figure 57). Whilst resins are not coastal bitumen, when identified they were collected. These samples were not analysed, for a summary of their geochemistry and correlation to Southeast Asia see Murray et al., (1994b).

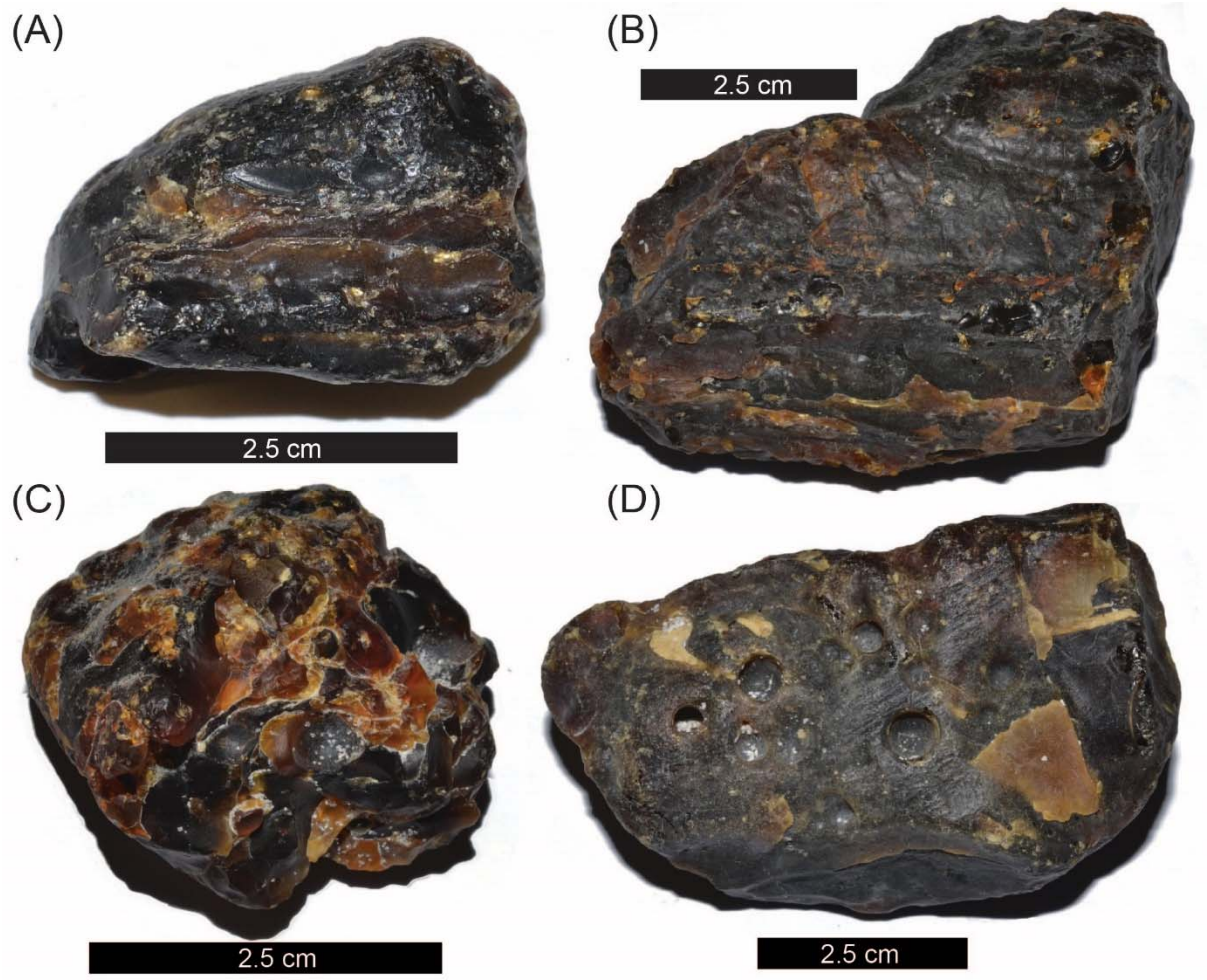

Figure 57: Examples of coastal amber/resins. (A) Sample W13/007555. (B) Sample W13/007645. (C) Sample W13/007761. (D) Sample W13/007555.

Sooty Bitumen

Sooty bitumens are a rarely encountered variety of coastal bitumen of unknown origin. These bitumens are solid but brittle and do not break with a conchoidal fracture. Upon collection or breaking these specimens leave a sooty residue on the nitrile gloves used for collection. Only three examples of sooty bitumen (Figure 58) were collected across the three annual surveys. Previous research by Padley (1995) considered the sooty bitumen anthropogenic in origin, attributed to oil slicks.

Figure 58: Sample W13/007518 of sooty bitumen.

Polycyclic Aromatic Hydrocarbons

Initially mistaken for coastal bitumen, three samples of pure polycyclic aromatic hydrocarbons (PAHs) were donated in 2015 and 2016 by local beachcomber Stuart Valladares. All specimens were collected from Avoid Bay and have been identified as pure, solid polycyclic aromatic hydrocarbons. These samples are visually similar to waxy bitumen, however they are solid, brittle and contain a series of brown fragments which on cursory examination may be mistaken for the surficial sand coating of a waxy bitumen (Figure 59).

Figure 59: Sample W13/007768C, comprised of pure polycyclic aromatic hydrocarbons.

Soft Bitumen

Coastal bitumen strandings are most commonly solid, with fresh examples being semi-solid and capable of deformation from a moderate amount of pressure. In 2016 two varieties of extremely soft bitumen were encountered on Sandy River (Figure 60A) and Number 1 and 2 Rocks (Figure 60B)

respectively. The strandings were extremely soft and sticky with a strong petroliferous odour and a surficial coating of sand. Collection of each specimen from the beach to store in a sample bag left an oil residue on the nitrile gloves used for collection and the specimen itself deforming in shape. Whilst the strandings encountered on Sandy River were smaller than those from Number 1 and 2 Rocks, the size difference should not be considered a diagnostic feature. Further classification of these strandings requires geochemical assessment.

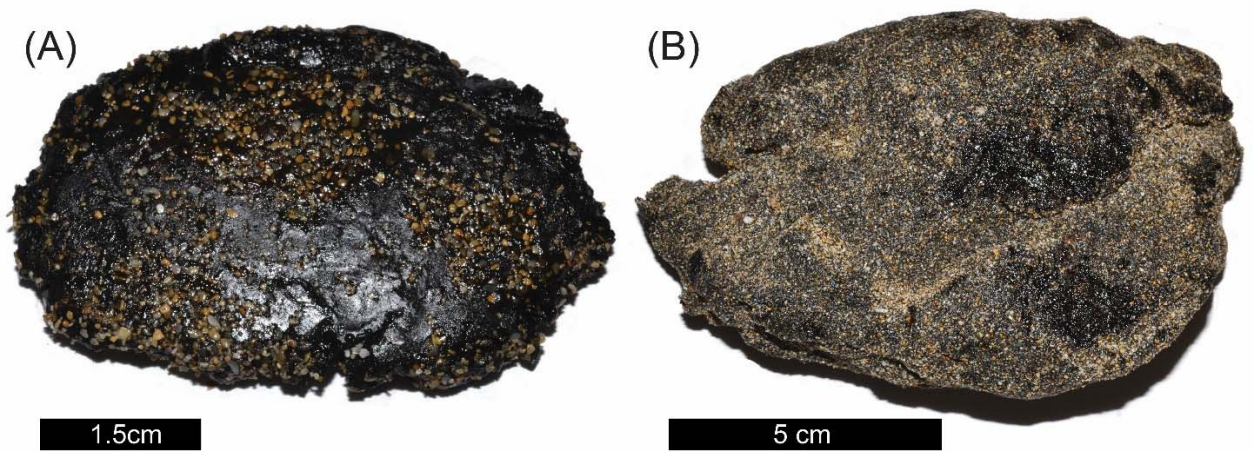

Figure 60: Examples of soft bitumen found in 2016. (A) Sample W13/007923 collected from Sandy River. Note the sample was flattened from storage in an aluminium sleeve. (B) Soft bitumen collected from Number 1 and 2 Rocks.

Bulk Geochemical Classification

Petroleum products are most commonly classified into oil families based on their source-specific biomarker geochemistry. However, given the large number of samples collected, a screening procedure was established to systematically identify key representative samples for detailed geochemical analysis.

A bulk geochemical screening procedure was developed to provide a straightforward classification scheme to broadly sub-divide coastal bitumen samples. All collected bitumen samples were assessed in terms in the following procedures:

- Percentage of carbon, hydrogen, nitrogen and sulphur (EA).
- Bulk carbon ($\delta^{13}C$) and sulphur ($\delta^{34}S$) isotopic composition (EA-IRMS)
- Whole oil GC-MS total ion chromatogram

Of these approaches, results from EA and EA-IRMS analyses were found to be far less conclusive in separating different types of coastal bitumen to be a viable as a screening tool and will not be discussed further. Therefore, all bitumen samples collected during the GABRP were classified into preliminary types based on their whole oil GC-MS results. This classification scheme is largely based on pattern recognition associated with key compounds and is summarised in Figure 61 and discussed below. The approach is successful in identifying the majority of coastal bitumen specimens collected

into several categories: asphaltites and waxy bitumen types I-IV (Figure 70). In addition rare outliers to these scheme are also discussed.

After assigning whole-oil classifications, a subset of representative samples from each preliminary oil family may be used for identification of sub-families based on source parameters.

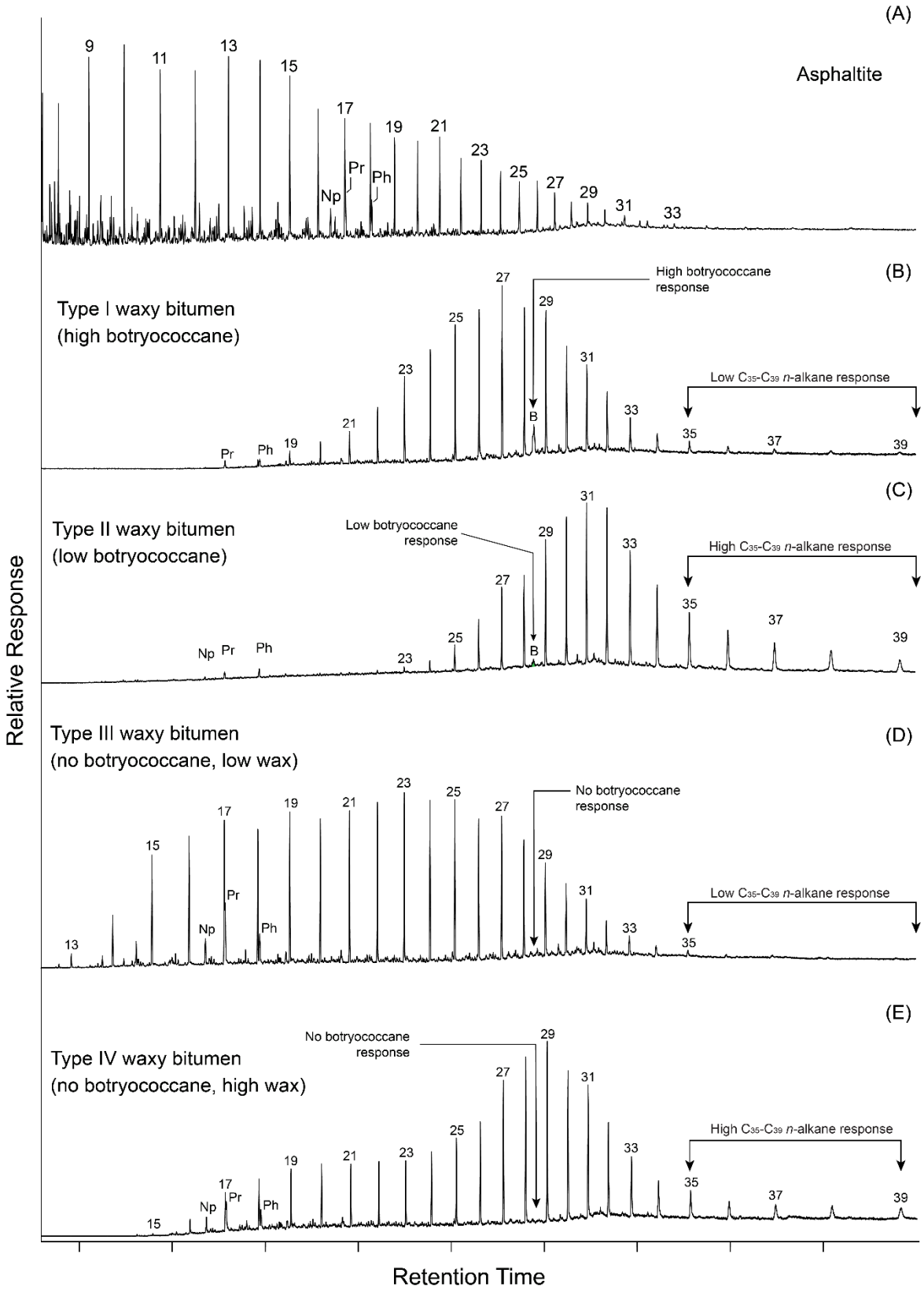

Figure 61: Whole-oil GC-MS total ion chromatograms of the freshest examples of the key whole-oil families for the South Australian coastal bitumen. (A) Asphaltite, sample W13/007976. (B) Type I waxy bitumen (high botryococcane), sample W13/007601. (C) Type II waxy bitumen (low botryococcane), sample W13/007615. (D) Type III waxy bitumen (no botryococcane, low wax), sample W13/007697. (E) Type IV waxy bitumen (no botryococcane, high wax), sample W13/007589.

Key Whole Oil Classifications for Coastal Bitumen Strandings

Asphaltite

The whole oil total ion chromatogram (TIC) for the freshest asphaltite collected is shown in Figure 61A. Asphaltites typically preserve *n*-alkanes as light as octane, nonane or decane (C8-C10 alkanes), with unaltered norpristane (Np), pristane (Pr) and phytane (Ph) and a Pr/Ph ratio of 1.1-1.3. These bitumens do not contain significant high molecular weight *n*-alkanes, with extremely low response peaks for *n*-alkanes > C31.

Type I Waxy Bitumen (High Botryococcane)

The whole oil TIC for the freshest Type I waxy bitumen is shown in Figure 61B. Type I waxy bitumens are the most clearly identifiable waxy bitumen due to their high abundance of the biomarker botryococcane, which elutes between the C28 and C29 *n*-alkanes. These bitumens show a decline in high molecular weight *n*-alkanes in towards C39. In the freshest sample collected, whilst pristane and phytane are present, these compounds have already experienced significant alteration and therefore should not be used for interpretation of source conditions or correlation. Biomarker analysis (discussed below) demonstrates the consistency of these bitumens as a single oil family. Therefore, identification of Type I bitumen may be made during whole oil screening.

Type II Waxy Bitumen (Low Botryococcane)

The whole oil TIC for the freshest Type II waxy bitumen is shown in Figure 61C. Type II waxy bitumens are recognisable by their low botryococcane content and high molecular weight *n*-alkanes in comparison to the Type I's. In the freshest examples collected, whilst pristane and phytane are present, they have experienced significant alteration and therefore should not be used for interpretation of source conditions or correlation.

Type III Waxy Bitumen (No Botryococcane, Low Wax)

The whole oil TIC for the freshest Type III waxy bitumen is shown in Figure 61D. Type III waxy bitumen are characterised by their lack of botryococcane and low abundance of high molecular weight *n*-alkanes (C35-C39).

Biomarker analysis (discussed below) demonstrates five potential oil families exist within the whole oil category of Type III waxy bitumen. Therefore, analysis of biomarkers from Type III waxy bitumen is required for complete classification. Although pristane and phytane are intact in certain examples of the Type III waxy bitumen, as numerous oil families exist on the basis of their biomarker geochemistry, it will not be discussed here.

Type IV Waxy Bitumen (No Botryococcane, High Wax)

The whole oil TIC for the freshest Type IV waxy bitumen is shown in Figure 61E. Type IV waxy bitumen are characterised by their lack of botryococcane and high abundance of high molecular weight *n*-alkanes (C35-39). Biomarker analysis (discussed below) demonstrates five potential oil families exist with these features in whole oil screening. Therefore, analysis of biomarkers from Type IV waxy bitumen is required for complete classification. Similar to the Type III waxy bitumen, due to the presence of multiple sub-families, assessment of the Pr/Ph ratio (when preserved) should only be applied after complete classification using diagnostic biomarkers.

Other Whole Oil Families

The whole oil classification scheme outlined above describes the majority of the different types of bitumen encountered along the South Australian coastline. However, there are also several outliers which fall outside of this scheme. These are samples which are either too degraded to conclusively identify, or strandings which were not encountered in all three of the annual surveys.

Unknowns

As coastal bitumen may spend years moving throughout the marine environment, some samples collected were too degraded to identify, with even the most recalcitrant compounds removed. Any samples which contained no clear identifying features in whole oil GC-MS was classified as 'Unknown'.

Unclassified High Wax Bitumen

Similar to highly degraded samples classified as 'Unknown'. Many coastal bitumen strandings were severely degraded to the point that a definitive whole oil classification could not be confidently applied. However, certain samples whilst heavily degraded, preserved strong response peaks for high molecular weight *n*-alkanes (e.g. Figure 62). These bitumen are most likely the extremely degraded end-members of the Type II and IV waxy bitumen, which also contain high molecular weight *n*-alkanes. However, as these samples cannot be confidently classified as either example, they were designated 'Unclassified high wax bitumen'.

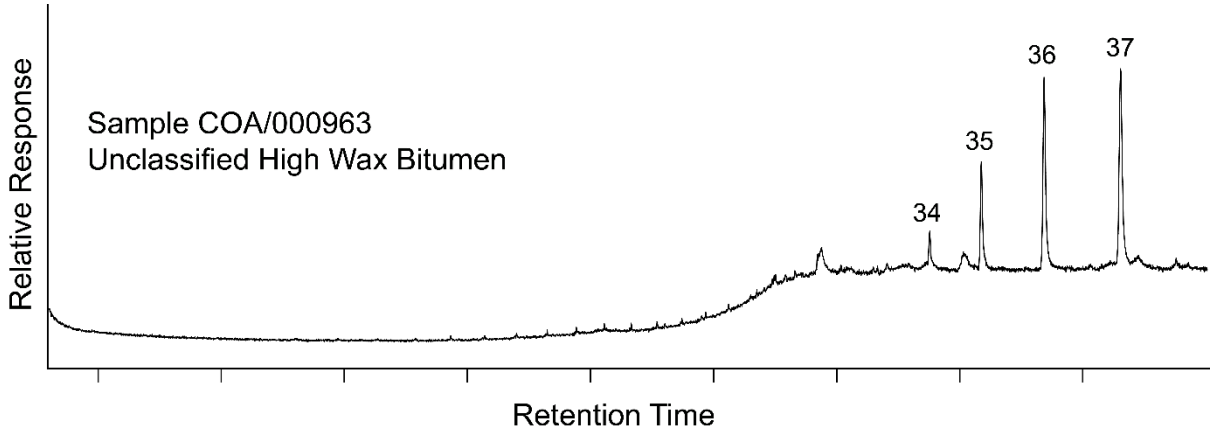

Figure 62: Whole oil GC-MS total ion chromatogram for unclassified high wax sample COA/000963. In this sample clear response peaks only remain for n-alkanes ≥ C34, limiting a descriptive classification.

Resinite / Amber

The total ion chromatogram of a resin/resinite is shown in Figure 63. Note that most resinites/ambers were identified visually and not analysed geochemically. However the chromatogram for bulk geochemical screening is provided here for reference in the event of future surveys.

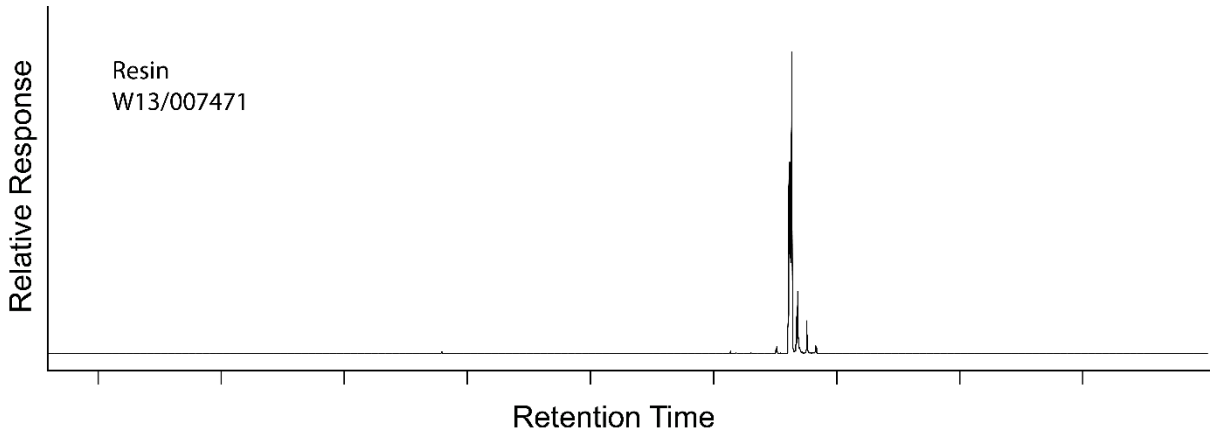

Figure 63: Whole oil GC-MS total ion chromatogram for resin sample W13/007471.

Sooty Bitumen

The whole oil total ion chromatogram of a sooty bitumen is shown in Figure 64. The sooty bitumen show a restricted n-alkane distribution with moderate degradation removing all *n*-alkanes < C15. These bitumen also lack high molecular weight *n*-alkanes > C34. After identification, sooty bitumen samples were not analysed in further detail.

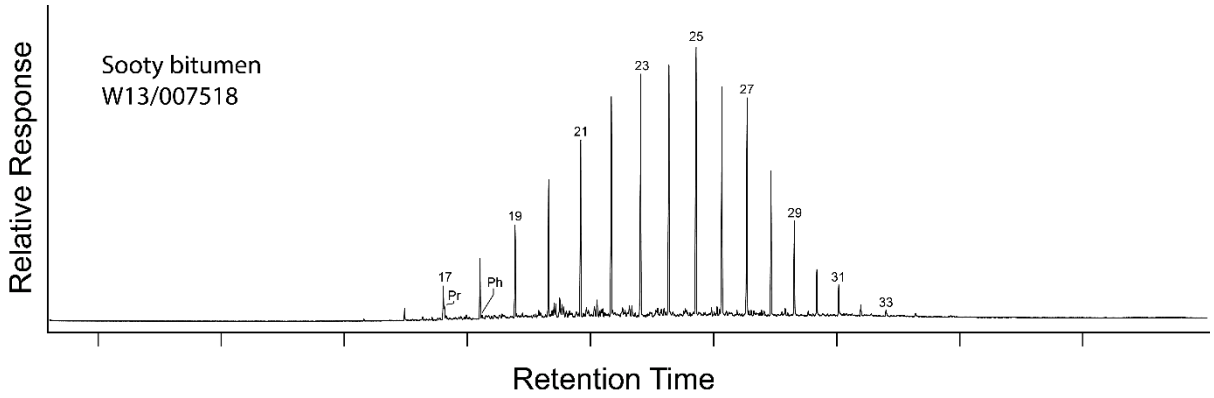

Figure 64: Whole oil GC-MS total ion chromatogram for sooty bitumen sample W13/007518.

Polycyclic Aromatic Hydrocarbons

The whole oil total ion chromatogram for a polycyclic aromatic hydrocarbon sample is shown in Figure 65. Polycyclic aromatic hydrocarbons are highly carcinogenic, usually occurring in low concentrations along with other organic compounds following incomplete combustion. Though health risks are primarily associated with inhalation/consumption of PAHs (e.g. Böstrom et al., 2002), the occurrence of such highly concentrated pieces of carcinogenic material occurring in the coastal environment is of concern.

Following identification as an outlier from the standard classification of bitumen and their restricted spatial distribution, these specimens were not analysed further. However, the origin of this material is likely anthropogenic and warrants further investigation from an environmental management

perspective. The whole oil chromatogram is provided here for reference in the event any future surveys encounter similar samples.

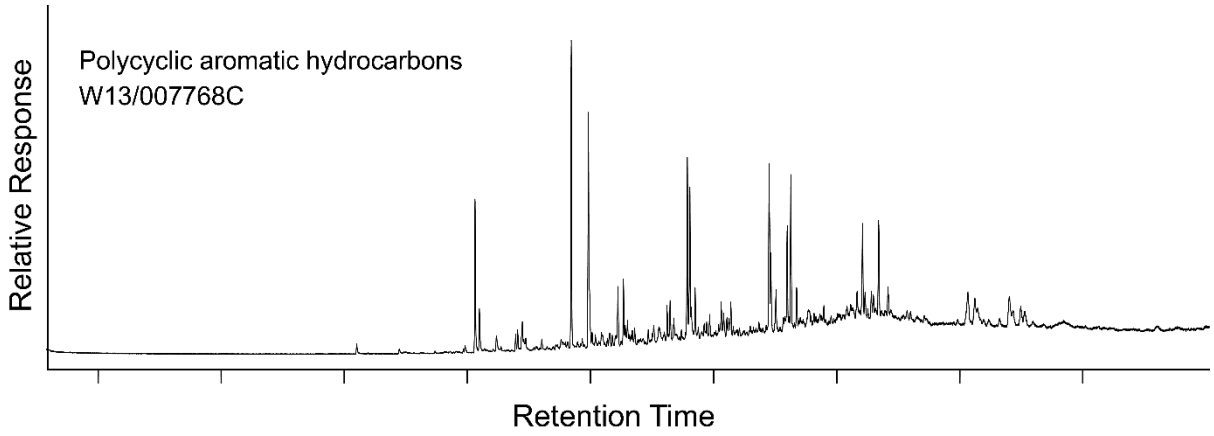

Figure 65: Whole oil GC-MS total ion chromatogram for polycyclic aromatic hydrocarbon sample W13/007768C.

Sandy River Soft Bitumen (2016 only)

The whole oil GC-MS total ion chromatogram for the Sandy River soft bitumen samples recovered only in 2016 is shown in Figure 66. These samples contain a characteristic biomodal UCM with a pristane and phytane maxima. This pattern is unlike the progressive degradation observed in coastal bitumen samples (discussed in the weathering section). Rather, this alteration is more commonly observed in biodegraded oils, tentatively suggesting these strandings may be the result of an amalgamated oil slick, rather than a seafloor bitumen seep. Given the biodegraded nature of these samples it is likely that the response peaks for pristane and phytane have experienced minor alteration.

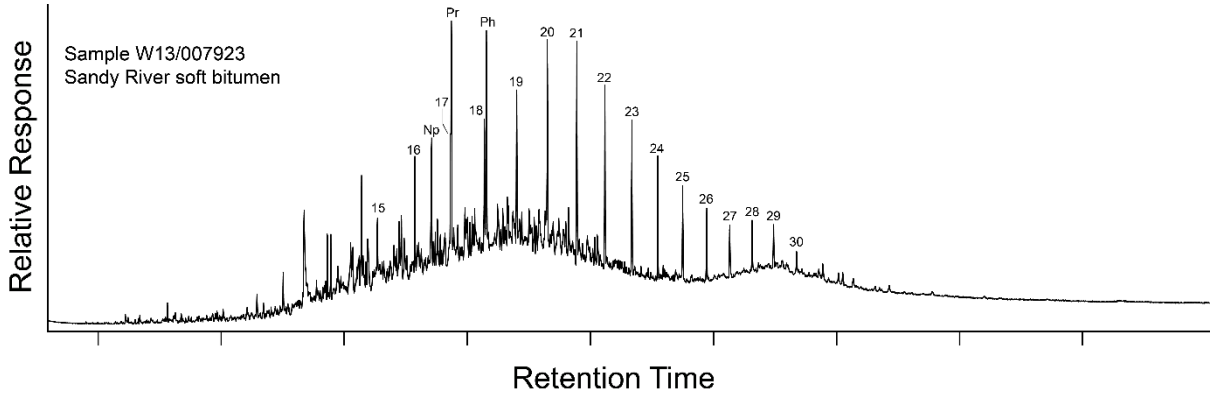

Figure 66: Whole oil GC-MS total ion chromatogram for Sandy River soft bitumen sample W13/007923.

Degraded Asphaltite (Tractor Beach in 2015/2016 only)

The whole oil GC-MS chromatogram for degraded asphaltite samples only found on Tractor Beach in 2015/2016 is shown in Figure 67. These samples are visually indistinguishable from asphaltites as they too break with a distinctive conchoidal fracture. However, the whole oil GC-MS chromatograms collected for these samples are not recognizable compared to other asphaltites due to extreme degradation removing almost all compounds. Whole oil GC-MS analysis required a splitless (undiluted) injection in order to obtain response peaks.

The identification of these bitumens as asphaltites relies heavily on their physical identification, most notably the diagnostic conchoidal fracture pattern. However, as these samples were relatively few in number, with 8 samples found in 2015 and 1 in 2016, all from Tractor Beach, they are considered outliers.

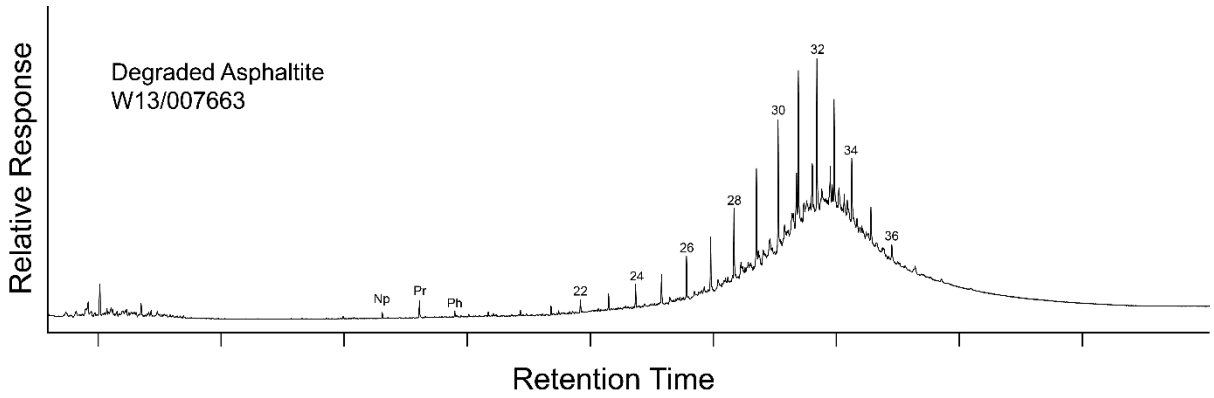

Figure 67: Whole oil GC-MS total ion chromatogram for degraded asphaltite sample W13/007663.

Number 1 & 2 Rocks Soft Bitumen (2016 only)

The whole oil total ion chromatogram for the soft bitumen collected from Number 1 and 2 Rocks in 2016 is shown in Figure 68. These strandings are extremely fresh, preserving low molecular weight gasoline range hydrocarbons such as octane (C8) or nonane (C9). Pristane and phytane appear unaltered in these samples, with a Pr/Ph ratio of ca. 0.8-0.9.

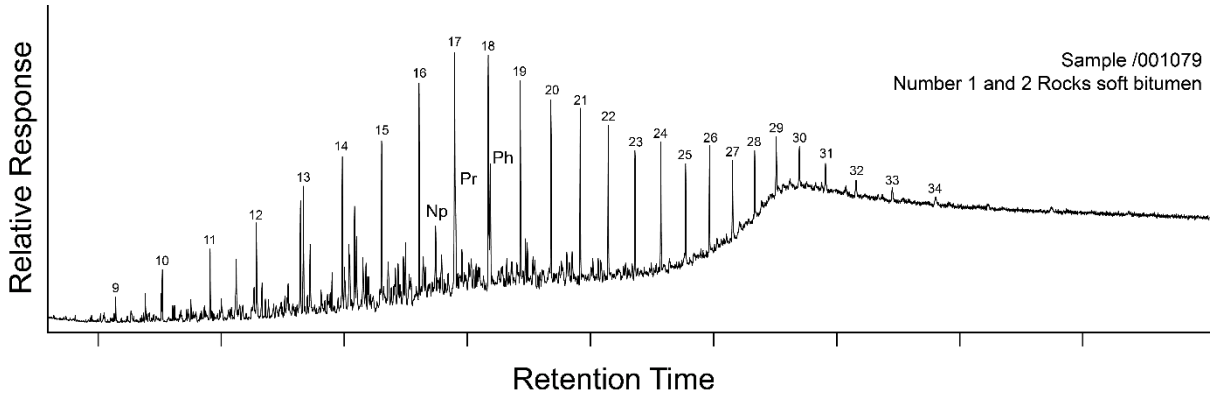

Figure 68: Whole oil GC-MS total ion chromatogram for Number 1 and 2 Rocks soft bitumen sample /001079.

Limitations of a whole-oil classification scheme

Analysis of the bitumen whole oil is designed only as a screening tool. It is important to note that this screening is insufficient to adequately identify the key characteristics of the parent petroleum systems. Thus, it is important to recognise that not all bitumen classified by the whole oil composition can be assumed to be interpreted as part of the same petroleum system, only that they share similar bulk geochemical characteristics.

The detailed interpretation of the parent petroleum system requires an assessment of source-specific biomarkers. However, analysing the biomarker geochemistry of the full suite of collected coastal bitumens is also not practical. Analysis of the whole-oil using GC-MS allows for a rapid screening procedure which separates bitumen samples into several broad types. Representative samples from each of these types were then selected for detailed assessment using biomarker analyses.

The type III and IV waxy bitumens are particularly vulnerable to misclassification without assessing their biomarker composition as most crude oils will lack the rare biomarker botryococcane.

BIOMARKER CHARACTERISATION

Statistical treatment and interpretation

Geochemical grouping

Biomarkers are a group of compounds, primarily hydrocarbons, found in oils, rock extracts, recent sediment extracts and soil extracts. What distinguishes biomarkers from other compounds in oil is that they can reasonably be called “molecular fossils”. Biomarkers are structurally similar to, and are diagenetic alteration products of specific natural products (compounds produced by living organisms). Hence biomarkers such as terpanes, hopanes and steranes can provide information on the organic matter type in the source rock, its lithofacies, the depositional environment, age and thermal maturity. (Table 17).

Table 17: Summary of selected biomarkers and their related source indicators.

Source information		Biomarker parameters	Comments
Organic matter inputs	Terregious	Oleanane, Lupanes, bisnorlupanes	Presence indicating angiosperm higher plant inputs to source rock (Moldowan et al., 1994)
		A-ring contracted oleanoids	Presence indicating inputs of angiosperm plants that evolved during the Late Cretaceous
		Bicadinanes, methylbicadinane	being derived from Dipterocarpaceae tree resins (Cox et al., 1986; van Aarssen et al., 1990)
		Taraxastane	Presence indicating inputs of mangroves (Ekweozor & Udo, 1988)
		C_{29} steranes	High abundances relative to total C_{27}-C_{29} steranes (Huang & Meinschein, 1979; Moldowan et al., 1985)
		Sterane/hopane	<1 indicating terrigenous and/or microbially reworked organic matter (Tssot & Welte, 1984)
		4-Methylsteranes	High abundances indicating lacustrine organic matter inputs (Peters et al., 2005)
	Lacustrine	Tetracyclic polyprenoids	High abundances indicating fresh-brakish water algal organic matter input (Holba et al., 2000, 2003)
		Botryococcane	Present indicating lacustrine-brackish source (Moldowan et al., 1980)
		C_{26}/C_{25} tricyclic terapnes	High (>1) in oils from source rocks depisted in lacustrine enviornment (Peters et al., 2005)
	Marine	24-*n* -propycholestanes	Presence indicating marine organic matter (Moldowan et al., 1990)
		Dinosteranes	Presence indicating marine dinoflagellate inputs (Peters et al., 2005)
		Sterane/hopane	≥1 indicating marine organic matter (Moldowan et al., 1985)
		C_{27} steranes	High abundances indicating algal inputs (Peters et al., 2005)
Source rock lithology	Carbonates	C_{24} tetracyclic terpane	High abundance in carbonate or evaporate source rock settings (Connan et al., 1986; Connan & Dessort, 1987; Mann et al., 1987; Clark & Philp. 1989)
		2α-methylhopane	High abundances in calcareous source rocks with high oxygen-producing cyanobacterial input (Summons et al., 1999)
		C_{29}/C_{30} αβ hopane	≥1 indicating carbonate source rocks (ten Haven et al., 1988)
	Shales	Diasteranes/steranes	High in clay-rich source rocks (Peters et al., 2005)
		Diahopane (C_{30}*)	Hign abundance in clay-rich source rocks (Peters et al., 2005)
		Rearranged hopanes (C_{29}Ts)	High abundances in clay-rich source rocks (Moldowan et al., 1991)
Depositional environment	Hypersaline	Gammacerance	High abundance in source rocks deposited under hypersaline depostional conditions (Sinninghe Damsté et al., 1995)
	Anoxic	C_{35}/C_{34} homohopane	>1 in oils from source rocks deposited under anoxic conditions (Peters & Moldowan, 1991)
		28.30-bisnorhopane	High in petroleum source rocks deposited in anoxic environment (Schoell et al., 1992; Moldowan et al., 1984)

Sample selection for chemometric statistical analysis

Sample selection was significantly influenced by the extent of biodegradation the samples had experienced as biodegradation results in alteration of components in petroleum by living organism which is a quasi-stepwise process. Saturated and aromatic biomarkers are biodegraded only after consumption of *n*-alkanes, most simple branched alkanes and some of the alkylated benzenes

(Seifert & Moldowan, 1979; Connan, 1984; Seifert et al., 1984). Hence, samples with unaffected biomarkers are preferable to be selected for chemometric statistical analysis. Based on the whole-oil chromatograms, some heavily biodegraded samples such as those with no or very low *n*-alkanes (Figure 69) or only C_{29}^{+}*n*-alkanes, were excluded from the statistical analysis. For the rest of the samples, considering the variation between interior and exterior of the samples which might be due to biodegradation or water washing, only interior and bulk samples (total of 114 samples) were chosen for the chemometric statistical analysis.

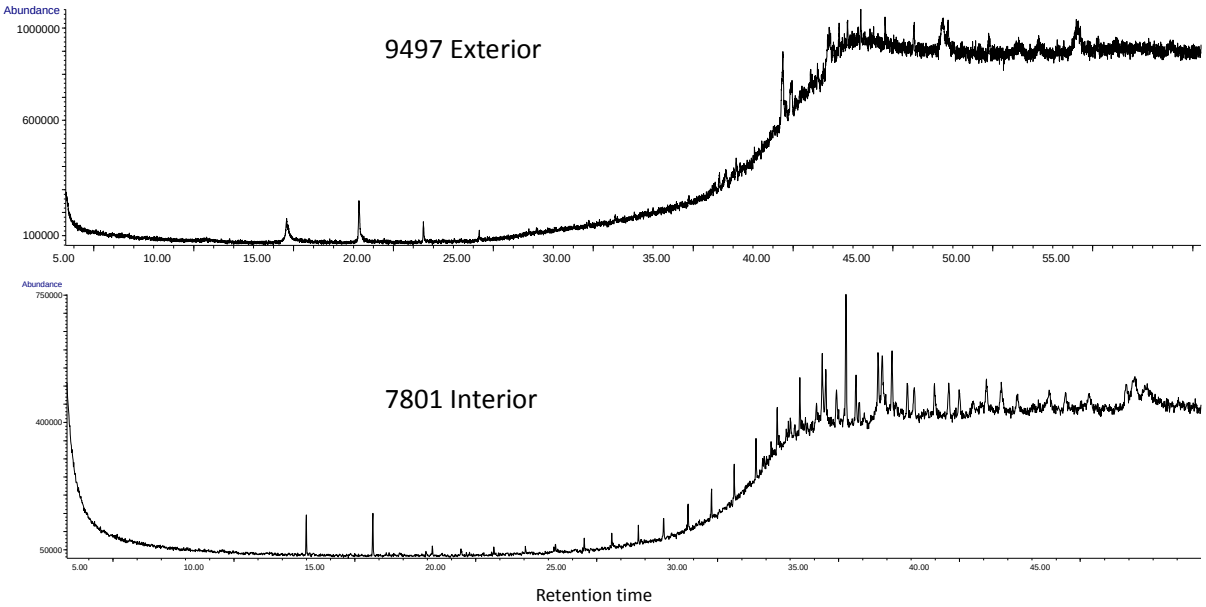

Figure 69: Total Ion chromatograms of representative whole oil samples which were heavily biodegraded.

Chemometrics is the use of multivariate statistics to recognize patterns and extract useful information from measured data (Kramer, 1998). Multivariate techniques treat all of the data simultaneously using matrix algebra, thus allowing the unique description of a sample by a point in space that has as many axes as variables. In chemometric exploratory data analysis, the data are processed and graphically displayed. Two of the most common techniques for chemometric exploratory data are hierarchical cluster analysis (HCA) and principal component analysis (PCA). The HCA dendrogram provides a simple view of groups of samples in the data set, where cluster distance is a relative measure of the degree of similarity among samples.

The statistical analysis of multivariate geochemical data in Figure 70 was completed using a commercial chemometrics program (Pirouette, Informetrix Inc. Woodinville, WA, USA). The HCA was completed using autoscale preprocessing, Euclidean metric distance, and incremental linkage with normalized data. The analysis included 32 source-related variables derived from the molecular distributions of hopanes and steranes which are not significantly affected by migration, biodegradation or thermal maturity. These parameters are listed in the Figure 70's caption. Based on this multivariate statistical analysis, the asphaltite and waxy bitumen samples were divided into seven groups with a similarity value of 0.58 (Figure 70). The groups were further divided into sub-groups with a similarity value of 0.8.

Biomarker characterization is discussed in the following section for eachgroup. Terpane and hopane (*m/z* 191), methylhopane (*m/z* 205), diasterane and sterane (*m/z* 217) and diasterane and tetracyclic polyprenoid (*m/z* 259) distributions of representative samples from each group are shown in each group discussion. The peak assignments are listed in Table 18 and Table 19.

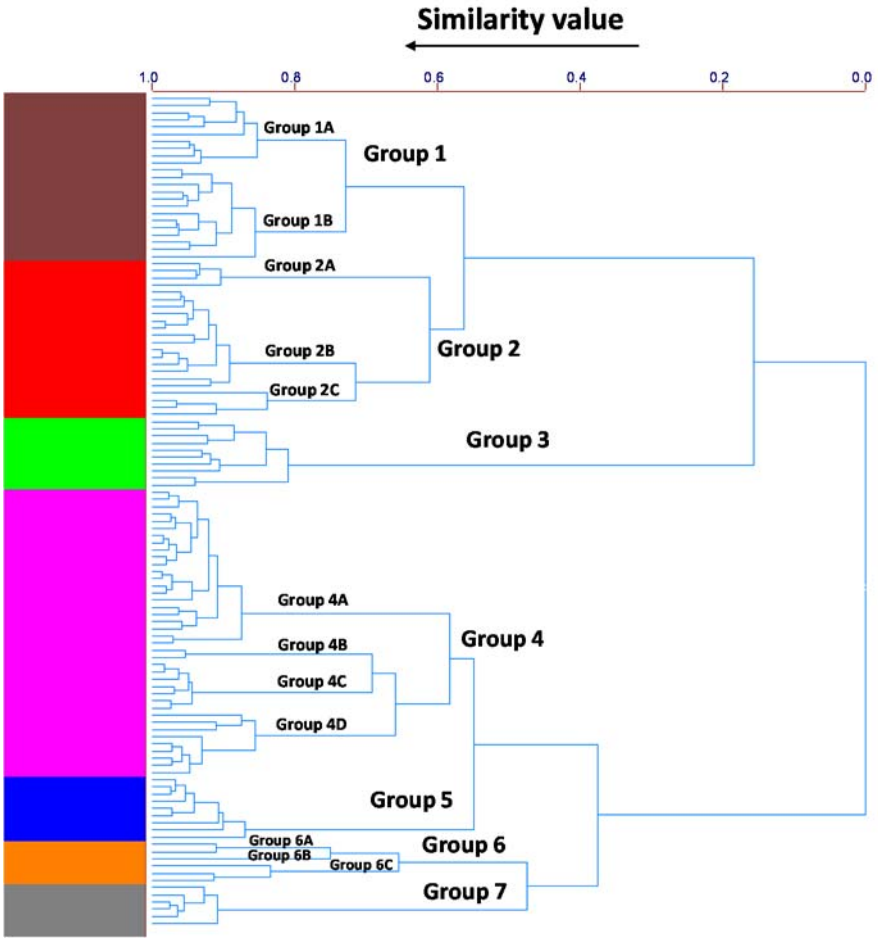

Figure 70: Dendrogram of the hierarchical cluster analysis (HCA) of 32 source variables showing different groups of asphaltite and waxy bitumen samples.

The source variables used for calculation of Euclidean distance (autoscale preprocessing, incremental linkage) are: **1**. C_{19}/C_{23} tricyclic terpanes, **2**. C_{22}/C_{21} tricyclic terpanes, **3**. C_{22}/C_{24} tricyclic terpanes, **4**. C_{24}/C_{23} tricyclic terpanes, **5**. C_{26}/C_{25} tricyclic terpanes, **6**. C_{24} tetracyclic/C_{23} tricyclic terpanes, **7**. C_{24} tetracyclic/C_{26} tricyclic terpanes, **8**. C_{23} tricyclic terpanes/ C_{30} αβ hopane, **9**. C_{24} tetracyclic terpane/ C_{30} αβ hopane, **10**. C_{24} bisnorhopane/ C_{30} αβ hopane, **11**. C_{29} αβ hopane/C_{30} αβ hopane, **12**. C_{30}* hopane/C_{30} αβ hopane, **13**. Oleanane/C_{30} αβ hopane, **14**. C_{30}-nor hopane/C_{30} αβ hopane, **15**. Ga/C_{30} αβ hopane, **16**. Ga/C_{31} αβ hopane R, **17**. C_{35} αβ hopane S/C_{34} αβ hopane S, **18**. C_{35} homohopane Index, **19**. C_{29}Ts/C_{29} αβ hopane, **20**. C_{27} ααα steranes 20 *R* (%), **21**. C_{28} ααα steranes 20 *R* (%), **22**. C_{29} ααα steranes 20 *R* (%), **23**. C_{27} diasteranes/ (diasteranes+steranes), **24**. (C_{21}+C_{22})/(C_{27}+C_{28}+C_{29}) steranes, **25.** C_{27} diasteranes/ steranes, **26.** C_{27} αββ steranes 20 *S+R* (%), **27**. C_{28} αββ steranes 20 *S+R* (%), **28**. C_{29} αββ steranes 20 *S+R* (%), **29**.C_{29}/C_{27} αββ steranes, **30**. Tricyclic/Pentacyclic terpanes, **31**. Steranes/Terpanes, **32**. Steranes/hopanes

Table 18: Peak assignments for terpanes in the *m/z* 191 and 205 mass chromatograms.

PEAK	TERPANE ASSIGNMENTS
19/3	C_{19} tricyclic terpane
24/4	C_{24} tetracyclic terpane

Ts	C_{27} 18α(H),22,29,30-trisnorneohopane
Tm	C_{27} 17α(H),22,29,30-trisnorhopane
28,30-BNH	C_{28} 28,30-bisnorhopane
25-nor	C_{29} 25-nor-17α(H)-hopane
C_{29}*	C_{29} 17α(H)-diahopane
C_{29} αβ	17α(H),21β(H)-30-norhopane
C_{29}Ts	18α(H)-30-norneohopane
C_{30}*	C_{30} 17α(H)-diahopane
C_{29} βα	17β(H),21α(H)-30-norhopane
Oleanane	18α(H)-oleanane (+ 18β(H)-oleanane)
C_{30} αβ	17α(H),21β(H)-hopane
30-nor	C_{30} to C_{34} 30-nor-17α(H)-hopanes
C_{30} βα	17β(H),21α(H)-hopane
C_{31} αβ 22*S*	17α(H),21β(H)-homohopane (22*S*)
C_{31} αβ 22*R*	17α(H),21β(H)-homohopane (22*R*)
G	Gammacerane
C_{32} αβ 22*S*	17α(H),21β(H)-bishomohopane (22*S*)
C_{32} αβ 22*R*	17α(H),21β(H)-bishomohopane (22*R*)
C_{33} αβ 22*S*	17α(H),21β(H)-trishomohopane (22*S*)
C_{33} αβ 22*R*	17α(H),21β(H)-trishomohopane (22*R*)
C_{34} αβ 22*S*	17α(H),21β(H)-tetrakishomohopane (22*S*)
C_{34} αβ 22*R*	17α(H),21β(H)-tetrakishomohopane (22*R*)
C_{35} αβ 22*S*	17α(H),21β(H)-pentakishomohopane (22*S*)
C_{35} αβ 22*R*	17α(H),21β(H)-pentakishomohopane (22*R*)
2α(Me)	2α-methylhopane
3β(Me)	3β-methylhopane
T, T1 and R	C_{30} bicadinanes of proven or inferred *trans-trans-trans* configuration
MeT	C_{31} methylbicadinanes
dO, dL and dU	A-ring degraded oleanane, lupane and ursane
BNO	bisnoroleanane
BNL	bisnorlupane

Table 19: Peak assignments for steranes, diasteranes and methylsteranes in the *m/z* 217 and 259 mass chromatograms and MRM chromatograms.

PEAK	STERANE, DIASTERANE AND METHYLSTERANE ASSIGNMENTS	ABBREVIATION

a	13β(H),17α(H)-diacholestane (20*S*)	C_{27} βα 20*S* diasterane
b	13β(H),17α(H)-diacholestane (20*R*)	C_{27} βα 20*R* diasterane
c	13α(H),17β(H)-diacholestane (20*S*)	C_{27} αβ 20*S* diasterane
d	13α(H),17β(H)-diacholestane (20*R*)	C_{27} αβ 20*R* diasterane
e	5α(H),14α(H),17α(H)-cholestane (20*S*)	C_{27} ααα 20*S* sterane
f	5α(H),14β(H),17β(H)-cholestane (20*R*)	C_{27} αββ 20*R* sterane
g	5α(H),14β(H),17β(H)-cholestane (20*S*)	C_{27} αββ 20*S* sterane
h	5α(H),14α(H),17α(H)-cholestane (20*R*)	C_{27} ααα 20*R* sterane
i	24-methyl-13β(H),17α(H)-diacholestane (20*S*)	C_{28} βα 20*S* diasterane
j	24-methyl-13β(H),17α(H)-diacholestane (20*R*)	C_{28} βα 20*R* diasterane
k	24-methyl-13α(H),17β(H)-diacholestane (20*S*)	C_{28} αβ 20*S* diasterane
l	24-methyl-13α(H),17β(H)-diacholestane (20*R*)	C_{28} αβ 20*R* diasterane
m	24-methyl-5α(H),14α(H),17α(H)-cholestane (20*S*)	C_{28} ααα 20*S* sterane
n	24-methyl-5α(H),14β(H),17β(H)-cholestane (20*R*)	C_{28} αββ 20*R* sterane
o	24-methyl-5α(H),14β(H),17β(H)-cholestane (20*S*)	C_{28} αββ 20*S* sterane
p	24-methyl-5α(H),14α(H),17α(H)-cholestane (20*R*)	C_{28} ααα 20*R* sterane
q	24-ethyl-13β(H),17α(H)-diacholestane (20*S*)	C_{29} βα 20*S* diasterane
r	24-ethyl-13β(H),17α(H)-diacholestane (20*R*)	C_{29} βα 20*R* diasterane
s	24-ethyl-13α(H),17β(H)-diacholestane (20*S*)	C_{29} αβ 20*S* diasterane
t	24-ethyl-13α(H),17β(H)-diacholestane (20*R*)	C_{29} αβ 20*R* diasterane
u	24-ethyl-5α(H),14α(H),17α(H)-cholestane (20*S*)	C_{29} ααα 20*S* sterane
v	24-ethyl-5α(H),14β(H),17β(H)-cholestane (20*R*)	C_{29} αββ 20*R* sterane
w	24-ethyl-5α(H),14β(H),17β(H)-cholestane (20*S*)	C_{29} αββ 20*S* sterane
x	24-ethyl-5α(H),14α(H),17α(H)-cholestane (20*R*)	C_{29} ααα 20*R* sterane
y	24-*n*-propyl-13β(H),17α(H)-diacholestane (20*S*)	C_{30} βα 20*S* diasterane
z	24-*n*-propyl-13β(H),17α(H)-diacholestane (20*R*)	C_{30} βα 20*R* diasterane
A	24-*n*-propyl-5α(H),14α(H),17α(H)-cholestane (20*S*)	C_{30} ααα 20*S* sterane
B	24-*n*-propyl-5α(H),14β(H),17β(H)-cholestane (20*R*)	C_{30} αββ 20*R* sterane
C	24-*n*-propyl-5α(H),14β(H),17β(H)-cholestane (20*S*)	C_{30} αββ 20*S* sterane
D	24-*n*-propyl-5α(H),14α(H),17α(H)-cholestane (20*R*)	C_{30} ααα 20*R* sterane
Ta	Tetracyclic polyprenoid Ta (Holba et al., 2000)	TPP Ta
Tb	Tetracyclic polyprenoid Tb (Holba et al., 2000)	TPP Tb

Group 1

Group 1 mainly consists of twenty two Type I and one Type IV waxy bitumen samples (Figure 71) with a similarity value of 0.72. The Type I waxy bitumens in this group contain a high abundance of botryococcane which is a fresh-brackish water green algal biomarker (Moldowan et al., 1980; McKirdy et al., 1986). The Type IV waxy bitumen samples in Group 1 contains no botryococcane. Group 1 was divided into two sub-groups, Group 1A and 1B.

The abundances of tricyclic terpanes are generally low in Group 1 samples (Figure 72) with C_{23} tricyclic terpane/ C_{30} $\alpha\beta$ hopane ranging from 0.03 to 0.18. The C_{24} tetracyclic terpane, a biomarker for principally carbonate or evaporite source rock settings (Connan et al., 1986; Connan & Dessort, 1987; Mann et al., 1987; Clark & Philp, 1989) and also originating from terrigenous organic matter (Philp & Gilbert, 1986), are present in low abundance (Figure 72) with the majority of C_{24} tetracyclic/C_{26} tricyclic terpane values ranging from 0.2 to 0.65. C_{26}/C_{25} tricyclic terpanes ratios range from 1.6 to 3.1, indicating derivation from lacustrine source rocks (Peters et al., 2005). Extended tricyclic terpanes (C_{28}-C_{36}) are present in low abundances in all the samples in Group 1. Similar extended tricyclic terpanes were described in De Grande et al., (1993) from saline lacustrine and marine carbonate source rock extracts.

C_{30} $\alpha\beta$ hopane is the dominant compound in the *m/z* 191 chromatogram (Figure 72) with C_{29}/C_{30} $\alpha\beta$ hopane ranging from 0.51 to 0.66, indicating that the source rocks for the Group 1 samples are not calcareous. High abundances of rearranged hopanes (Ts and C_{29}Ts) and diahopane (C_{30}*) are present in all samples in this group (Figure 72), indicating a sub-oxic/clay-rich depositional environment for their source rocks (Moldowan et al., 1991; Peters et al., 2005). Ts is much more abundant than Tm. C_{29}Ts/C_{29} $\alpha\beta$ hopane ranges from 0.27 to 0.42 and C_{30}*/C_{30} $\alpha\beta$ hopane ranges from 0.14 to 0.26.

Relatively high abundances of C_{31}-C_{34} 2α-methylhopanes and C_{31}-C_{33} 3β methylhopanes present in the Group 1 samples (Figure 73) probably indicate inputs of oxygen-producing cyanobacteria (Summons and Jahnke, 1990) and aerobic methanotrophic bacteria (Burhan et al., 2002; Farrimond et al., 2004).

Oleanane, a biomarker for angiosperm higher plants that radiated during the Middle Jurassic to Late Cretaceous or younger (Moldowa*n* et al*.,* 1994; Bell et al., 2005; Zheng & Wang, 2010), is present in relatively low abundance (Figure 72) with oleanane/C_{30} $\alpha\beta$ hopane ranging from 0.08 to 0.24.

Bicadinanes are common biomarkers in Southeast Asian oils with fluvio-deltaic source rocks which are interpreted to be derived from source rocks containing resins of the Dipterocarpaceae family (van Aarssen et al., 1990) or non-tropical angiosperm families (van Aarssen et al., 1994; Murray et al., 1994). Bicadinanes are present in the Group 1 samples (Figure 72).

C_{29} $\alpha\beta\beta$ steranes are relatively low in abundances relative to C_{27} $\alpha\beta\beta$ steranes in the majority of the Group 1 samples (C_{29}/C_{27} $\alpha\beta\beta$ steranes = 0.45-86) with the exception of three samples (7857A, 7528 and 7521) with C_{29}/C_{27} $\alpha\beta\beta$ steranes = 1.22-1.36 indicating that the majority of the Group 1 samples were likely derived from source rocks with more algal inputs. 24-*n*-Propycholestanes that are diagnostic compounds for marine organic matter input (Moldowan et al., 1990) are absent in the Group 1 samples but 4-methylsteranes, biomarkers for lacustrine dinoflagellate algal inputs when abundant (Peters et al., 2005), are present in high relative abundances based on MRM data. Low sterane/hopane ratios (0.05-0.1) indicate terrigenous or microbially reworked organic matter inputs

C_{27} diasteranes are present in relatively high abundances compared to the regular steranes (Figure 74) with C_{27} dia/(dia+reg) steranes ratios ranging from 0.64 to 0.78, indicating that the Group 1 samples were possibly derived from clay-rich source rocks deposited in an oxic depositional environment (Peters et al., 2005). This is consistent with high abundances of rearranged hopanes and diahopanes.

A doublet of late-eluting peaks identified as the tetracyclic polyprenoids Ta and Tb in m/z 259 mass chromatogram, biomarkers for freshwater lacustrine green algal input when present in high abundances (Holba et al., 2000, 2003), are present in high abundances in the Group 1 samples (Figure 75).

In summary, the Group 1 samples were likely derived from lacustrine shale deposited in a sub-oxic depositional environment with significant lacustrine algal and bacterial inputs and minor terrestrial contributions from angiosperm higher plants (Table 20).

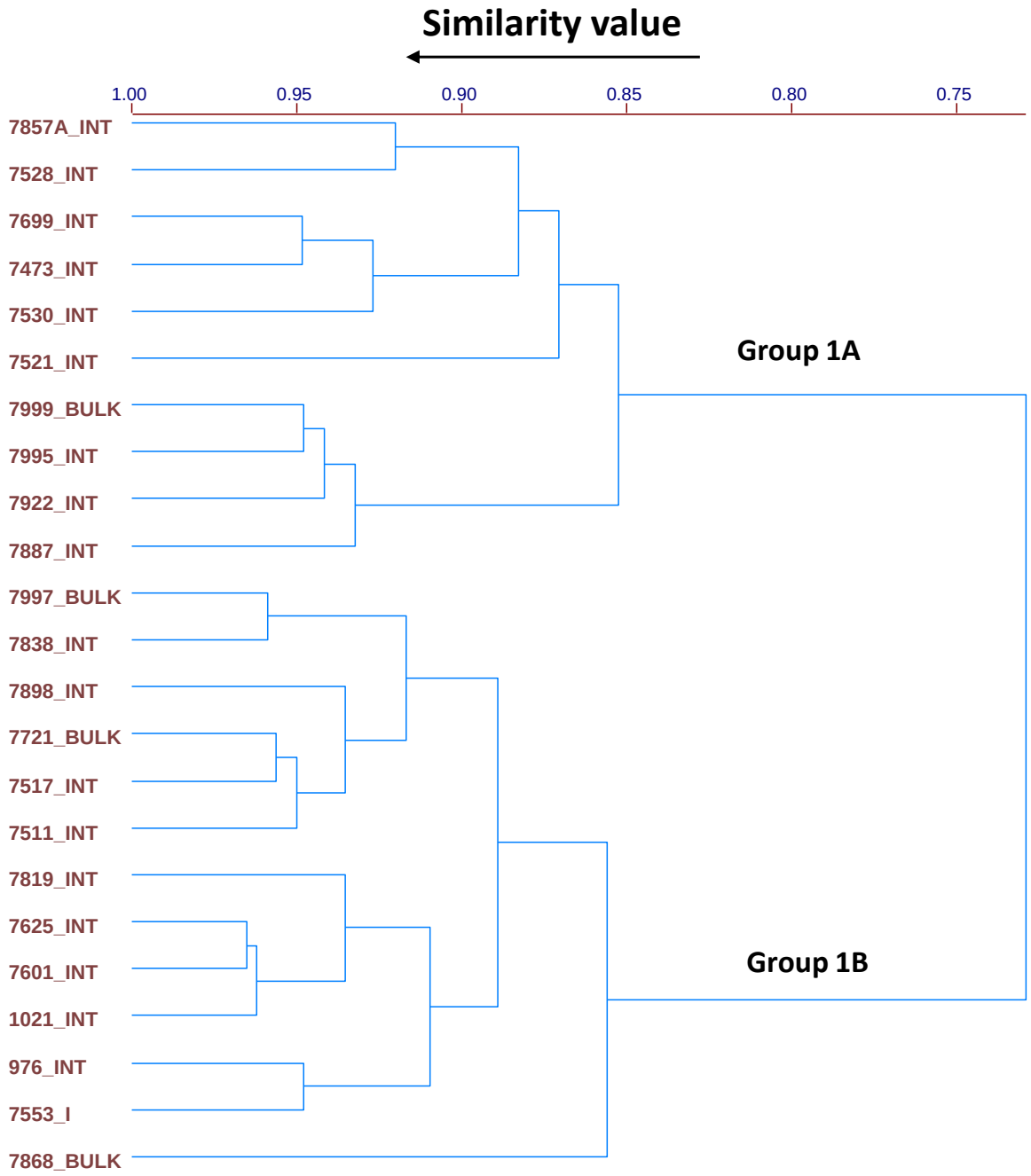

Figure 71: Partial dendrogram of the hierarchical cluster analysis of Group 1 samples in Figure 70.

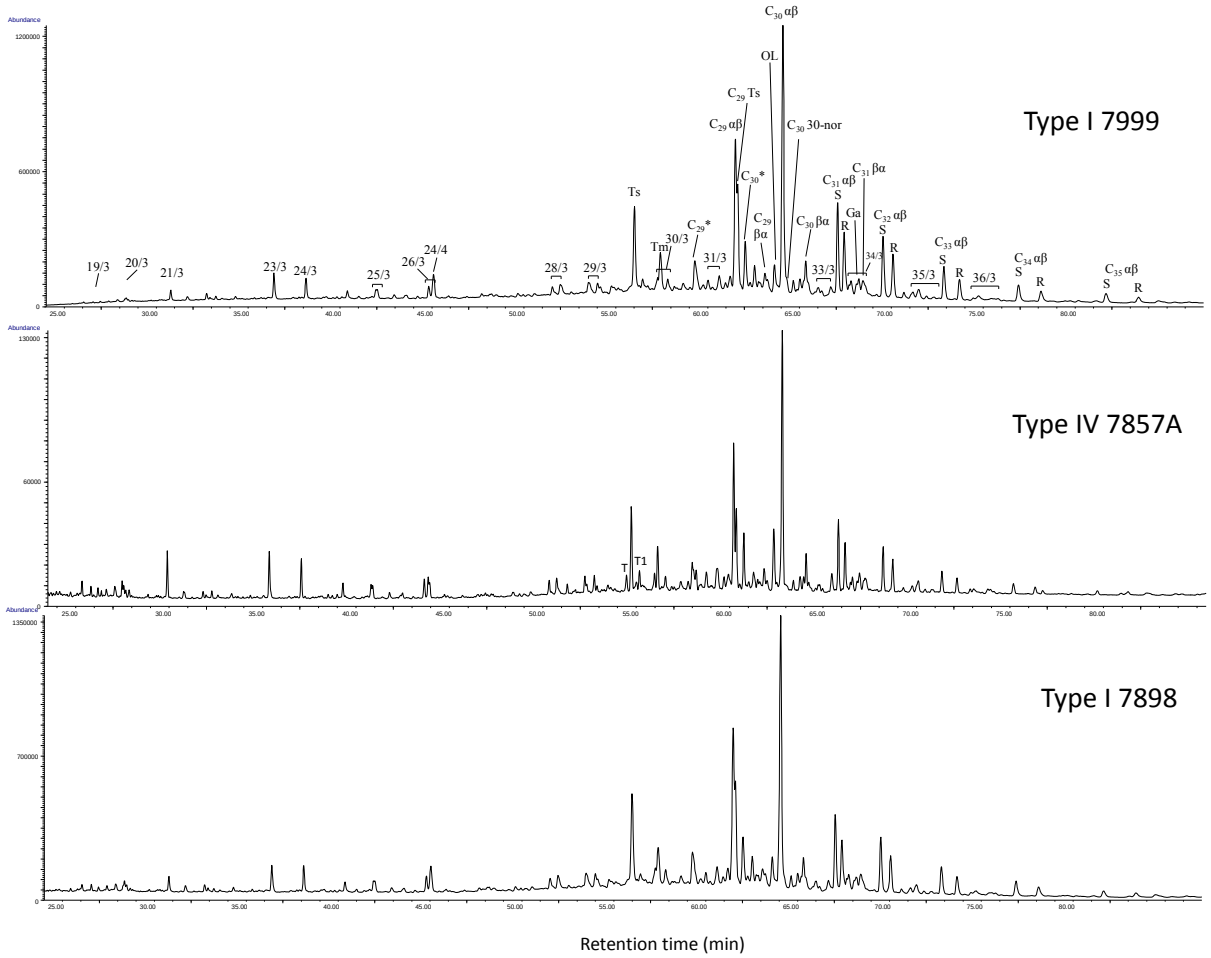

Figure 72: Partial *m/z* 191 mass chromatograms of representative Type I waxy bitumens (7898 and 7999) and Type IV waxy bitumen (7857A) in Group 1 showing the distribution of tricyclic terpanes and hopanes. For peak identifications refer to table 18.

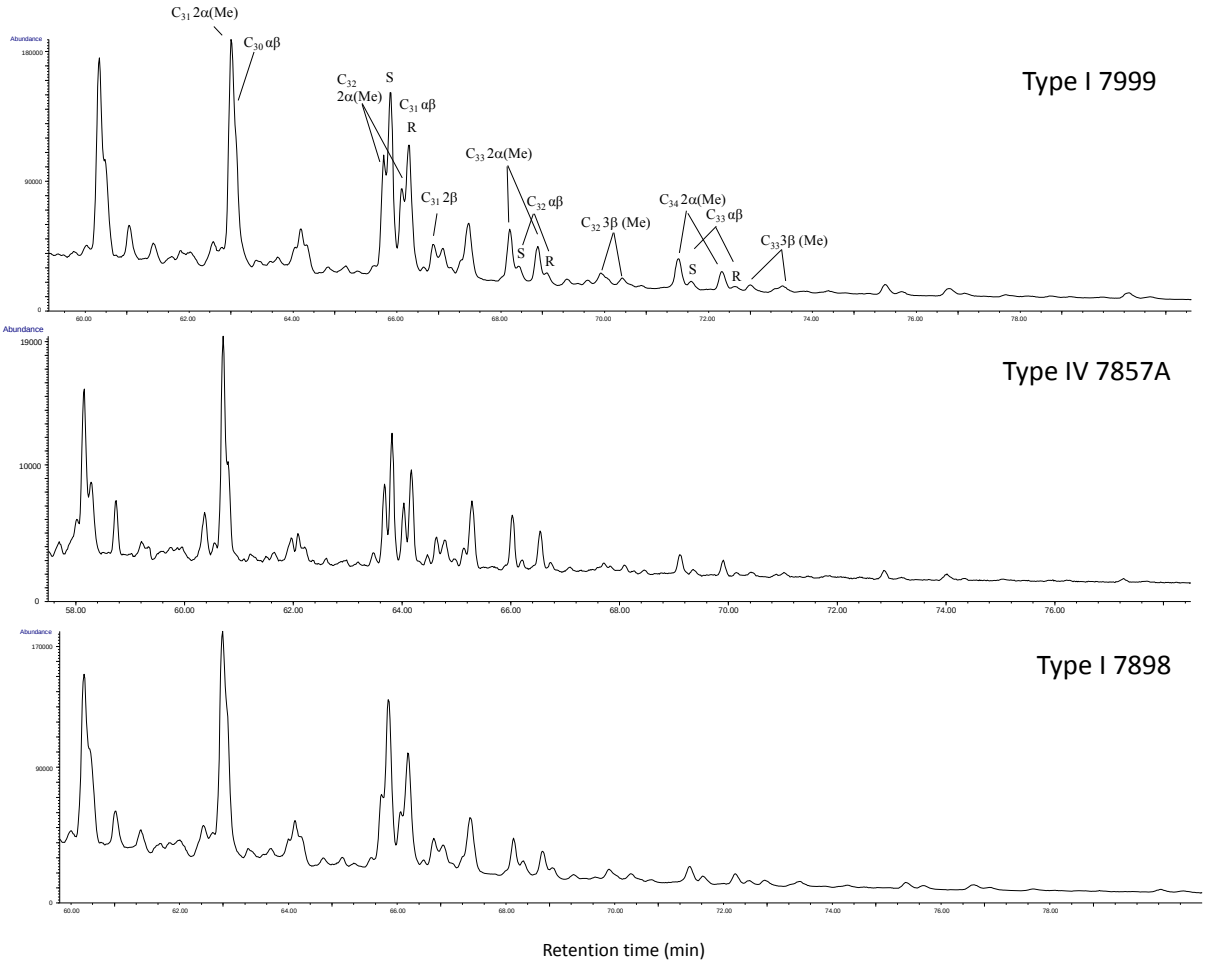

Figure 73: Partial *m/z* 205 mass chromatograms of representative Type I waxy bitumens (7898 and 7999) and Type IV waxy bitumen (7857A) in Group 1 showing the distribution of methylhopanes. For peak identifications refer to table 18.

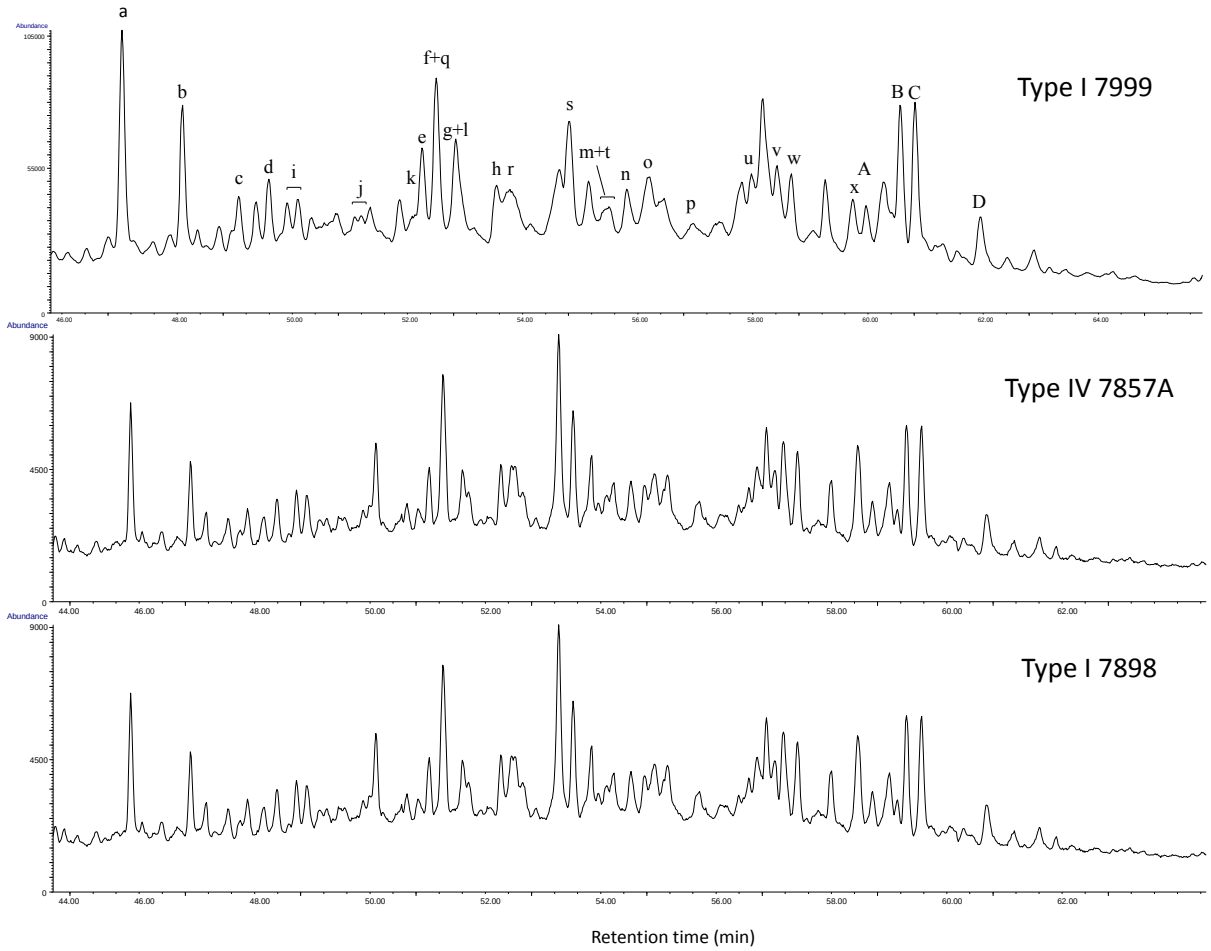

Figure 74: Partial *m/z* 217 mass chromatograms of representative Type I waxy bitumens (7898 and 7999) and Type IV waxy bitumen (7857A) in Group 1 showing the distribution of steranes and diasteranes. For peak identifications refer to table 19.